2010

Determination of Equilibrium binding constants for LPS interaction with TLR4

Santhoshi P. Dixit
West Virginia University

Determination of Equilibrium binding constants for LPS interaction with TLR4

Santhoshi P. Dixit

Thesis submitted to the

College of Engineering and Mineral Resources

at WEST VIRGINIA UNIVERSITY

in partial fulfillment of requirements

for the degree of

MASTER OF SCIENCE

in

Chemical Engineering

Advisor

Dr. David J Klinke

Committee Members

Dr. David J. Klinke

Dr. Charter D. Stinespring

Dr Robin S. Farmer

Morgantown, West Virginia

2010

Keywords: Innate immunity, Lipopolysaccharide, Toll-like receptors, TLR-4, SDS-PAGE, Flow cytometry, Trypan blue

ABSTRACT

Determination of LPS-TLR4 binding constants for LPS interaction with TLR4

Santhoshi Dixit

Toll-like receptors (TLRs) are the best characterized Pathogen Recognition Receptors (PRRs) and are directly responsible for initiating an appropriate defense against bacterial and viral infection. Among all the TLRs known, only TLR4 is able to activate both MyD88-dependent induction of genes encoding inflammatory molecules and TRIF-dependent production of type I interferon. Therefore, in this study we report the binding of TLR4 by Lipopolysaccharide (LPS) which is the component on the cell-wall of gram-negative bacteria. Binding of LPS is a prerequisite for the activation of Toll-like receptor 4 (TLR4) by LPS which increases the expression of critical proinflammatory cytokines that organize potent immune responses. The binding of LPS to TLR4 was studied using IC21 mice macrophage cell line and fluorescently labeled LPS molecule, called FITC-LPS by flow cytometry. The series of cell staining experiments were performed, which included binding of FITC-LPS to TLR4 at different temperatures as temperature influences cellular trafficking of TLR4. Since, trafficking or internalization of LPS depends on its aggregation behavior; the molecular state of LPS under experimental conditions is detected using SDS-PAGE. Trypan blue was used to identify surface bond versus internalized FITC-LPS.

DEDICATION

This thesis is dedicated to my grandfather, who taught me to that the best kind of knowledge to have is that which is learned for its own sake. It is also dedicated to my parents, who taught me that even largest task can be accomplished if it is done one step at a time.

ACKNOWLEDGEMENT

I would like to thank all people who have helped and inspired me during my master's study.

I especially want to thank my advisor Dr. David J. Klinke, for his guidance during my research and study, at West Virginia University. His perpetual energy and enthusiasm in research had motivated all his advisees, including me. In addition, he was always accessible and willing to help his students with their research. As a result, research life became smooth and rewarding for me.

I was delighted to interact with Dr. Rodney Brundage and Dr. Kathyleen Brundage, who supported me throughout my research work.

All my lab buddies made it a convivial place to work. In particular I would like to thank Dr. Yogesh Kulkarni and Viviana Suarez for their friendship and help during the lab work. All other folks had inspired me in research through our interactions during the long hours in the lab. Thanks

My deepest gratitude goes to my family for their unflagging love and support throughout my life; this dissertation is simply impossible without them. I am indebted to my father, Ashok Dixit, for his care and love. I cannot ask for more from my mother, as she is simply perfect. I have no suitable word that can fully describe her everlasting love to me. I remember many sleepless nights with her accompanying me when I was studying for examinations. I remember her constant support when I encountered difficulties and I remember, most of all, her delicious dishes. Mother, I love you.

The generous support from my best friend Ramanjaneyulu Katta is greatly appreciated. He was the person who stood beside me at toughest times.

Last but not least, Thanks to God for my life through all tests in the past seven years. You have made my life more bountiful. May your name be exalted, honored and glorified.

Table of Contents

List of Figures

List of Tables

Chapter 1. Introduction

The living organism contains an amazing array of systems to protect it from invading pathogens -called the immune system. The immune system is complex and interesting. Higher animals have two types of immunity. The first line of defense is called innate immunity; adaptive immunity is the second line of defense against infections. Innate immunity is responsible for defense against bacterial antigens. Lipopolysaccharide or LPS is found on the cell walls of gram negative bacteria such as *Escherichia coli*. LPS is recognized by innate immune system resulting in an inflammatory response. Front-line anti-microbial defense is accomplished by the innate immune system with the help of pattern recognition receptors (PRRs), such as Toll-like receptors, in early detection of pathogens. There are several types of PRRs including complement, glucan, mannose, scavenger, and toll-like receptors, each bind specific pathogen associated molecular patterns (PAMP). PAMPs are the broad classes of pathogens which express a set of class-specific, mutation resistant molecules. PAMPs include formulated peptides, and diverse bacterial cell wall components, such as lipopolysaccharide (LPS), lipopeptides, peptidoglycans, and teichoic acids.

Among all the TLRs, TLR4 is generally considered as a LPS receptor. TLR4 is expressed by B cells, dendritic cells, monocytes, macrophages and T cells. Among all these, macrophages are the cells which express high levels of TLR4, therefore macrophage cells are used to study the binding of LPS. The purpose of this study is to investigate the equilibrium binding constants of LPS to TLR4 of IC21 mice macrophage cells. The stimulation of TLR4 by LPS increases the expression of critical pro-inflammatory cytokines that are requisite to induce potent immune responses. LPS-TLR4 signaling has been intensively studied in past few years. LPS is mostly studied because it is a well characterized PAMP in which Lipid A portion is invariant and is present in every species of bacteria, but the O antigen portion is variant. And also LPS is found to

exhibit aggregation behavior in culture medium, so effective molecular weight of LPS during interaction with TLR4 is to be determined. SDS-PAGE is the proposed method to analyze LPS. TLR4 is chosen among all TLRs because TLR4 is the only TLR that can activate both MyD88-dependent induction of genes encoding inflammatory molecules and TRIF-dependent production of type I interferon. Therefore LPS when encountered by macrophages initiates a cascade of events resulting in the release of inflammatory cytokines and tissue factors. In this study, we investigate the kinetics involved in LPS-TLR4 binding because, we believe, the upstream binding processes directly affect the downstream signaling processes and the release of transcription factors and cytokines. Therefore, once LPS is analyzed, its interaction with TLR4 can be investigated and quantified.

Chapter 2. Literature Survey

2.0 Innate immunity

The immune system is composed of two major subdivisions; the innate and the adaptive immune system. The innate immune system provides early defense against pathogen invasion and it alerts the adaptive immune system about the pathogen invasion.[1] Each of the major subdivision has both cellular and humoral components by which they carry out their protective function. In addition, innate immune system has anatomical features that functions as barriers to infection. Although these two arms of the immune system have distinct functions, there is interplay between these systems (i.e., components of the innate immune system influence the adaptive immune system and vice versa).

There are two phases to the immune response: pathogen recognition and pathogen removal. Although the innate and adaptive immune systems both function to protect against invading organisms, they differ in a number of ways. The adaptive immune system requires some time to react to an invading organism, whereas the innate immune system includes defenses that are mostly present and ready to be mobilized upon infection. Second, the adaptive immune system is specific against new antigens identified as dangerous. In contrast, the innate immune system reacts to a small subset of patterns encoded within the genome and does not change. Finally, the adaptive immune system demonstrates immunological memory. It "remembers" that it has encountered an invading organism and reacts more rapidly on subsequent exposure to the same organism. In contrast, the innate immune system does not demonstrate immunological memory.

The innate immune system contains anatomical barriers such as skin, mucous membrane, saliva etc. However, when anatomical barriers are breached by tissue damage, inflammatory and cellular barriers come into play. [2] The cells that mediate innate immune response include macrophages, neutrophils, eosinophils, mast cells and natural killer cells. Pathogen recognition by innate immune system occurs through PRRs found in all cells of the innate immune system. These PRRs recognize the broad spectrum of molecular patterns PAMPs found in pathogens but not in the host. A particular PRR can

recognize a molecular pattern that may be present on a number of different pathogens enabling the receptor to recognize a variety of different pathogens.

2.1. Macrophages

Macrophages are the key players in the immune response to foreign invaders such as infectious microorganisms. Blood monocytes migrate into the tissues of the body and there evolve into macrophages. They are found in almost every tissue in the body, where they participate in various biological processes, ranging from development, to bone remodeling and wound healing. They express full repertoire of functions; they detect, ingest and destroy infectious agents; they initiate T-cell responses by antigen presentation, and they act as effector cells for both humoral and cell mediated responses. Macrophages express a broad range of plasma membrane receptors that mediate their interactions with natural and altered-self components of the host as well as a range of microorganisms. Macrophages express several receptor families responding to specific ligands and performing specific functions. Among which toll-like receptors respond to LPS. Recognition is followed by surface changes, uptake, signaling and altered gene expression, contributing to homeostasis, host defense, innate effector mechanisms, and the induction of acquired immunity.[3]

Two major classes of pattern recognition receptors exist in macrophages; endocytic pattern-recognition receptors and signaling pattern recognition receptors. Endocytic pattern-recogniton receptors are found on the phagocytic cells (neutrophils, monocytes and macrophages); these receptors attach microorganisms to phagocytes leading to engulfment and destruction. These include mannose receptors, scavanger receptors, opsonin receptors and N-formyl-met receptors. Signaling pattern-recognition receptors bind to PAMPs and promote the synthesis and secretion of intracellular regulatory molecules called as cytokines which are necessary to initiate innate immunity and adaptive immunity.[4] A series of signaling PRRs are found on the macrophages and

dendritic cells, these are known as toll-like receptors (TLRs). These receptors play an important role in induction of innate immunity and adaptive immunity. On binding of PAMPs to its TLR, a signal is transmitted to the host cell's nucleus leading to the induction of pro-inflammatory cytokines. These cytokines in turn bind to the cytokine receptors present on other defense cells such as cells of the adaptive immunity, thus initiating the induction of adaptive immunity.[3]

2.2. Lipopolysaccharide

Fever was one of the first recorded physical findings in medicine. Early investigators hypothesized that inducer of fever were physical entities and named them pyrogens, derived from the Greek root pyr, meaning fire. Then there was a controversy in stating fever as a disease or a host defense mechanism against illness. Albrecht von Haller, a pioneer in the field of LPS showed that decomposing tissue could induce fever when re-injected intravenously.[5] In 1892, Richard Pfeiffer published that *Vibrio cholera* had a toxin "closely attached to, and probably an integral part of, the bacterial body".[5] This came at a time when most scientists believed pyrogens to be secreted proteins like the other known bacterial toxins. Pfeiffer is credited with coining the term endotoxin (although he never published it), which is still used today.[6]

Endotoxin was first purified around by Andre Boivin and Lydia Mesrobeanu using a trichloroacetic acid (TCA)-based method. Soon after, Walter T.J. Morgan and Walther F. Goebel used organic solvents and water to purify endotoxin. Both groups found endotoxin to be composed of lipid and polysaccharide with very little if any associated protein.[5]

The bacterial endotoxin lipopolysaccharide (LPS) is the major constituent of gram-negative bacteria that activates TLRs. LPS consists of three covalently linked domains (Fig. 1). Lipid A (endotoxin), the core region and the O antigen polymer. Studies in several different laboratories determined that O antigen was a complex of

polysaccharide, composed of repeating units of five to eight monosaccharides (galactose, rhamnose, mannose and abequose in S.*tymphimurium*) that varies from strain to strain.[7] Not much is known about the biological activities of the outer core region of LPS, but it is believed that both the outer and inner core carry epitopes for antibodies.[8] Determining the structure of the extracted lipid was considerably more difficult than structuring either the core or O-antigen and it wasn't until 1983 that Takayama and colleagues published the complete structure and correct structure of lipid A.[9] The fatty acid composition of lipid A was first described in *E.coli.* A total of six fatty acids chains are attached to the lipid A backbone, two via amide linkages and four via ester linkages. Lipid A functions as the hydrophobic anchor for LPS in the outer membrane and is the bioactive component responsible for some of the pathophysiology, associated with severe Gram-negative infections

The most significant thing is the identification of TLR4 as a signaling receptor for LPS.[10] LPS is the most potent stimulator of macrophage derived cytokine secretion.[11] This excessive stimulation can lead to septic shock. Septic shock is the leading cause of deaths in hospitalized patients. Macrophage–derived cytokines especially tumor necrosis-alpha (TNFα) and interleukin-1 (IL-1) are showed to be involved in septic shock.[12, 13, 14]

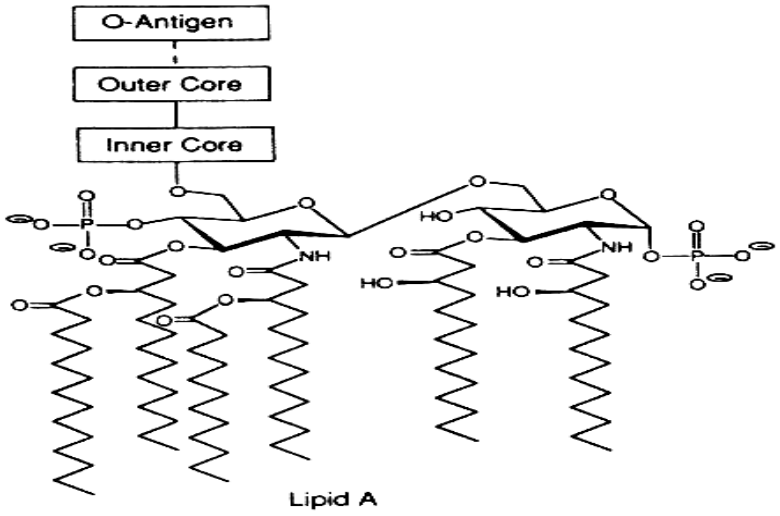

Figure 1. General structure of LPS. LPS of Enterobacteriaceae consists of three covalently linked domains: the lipid A moiety serves as the hydrophobic anchor for LPS

in the outer most bacterial membranes and confers endotoxic properties to the LPS, the core region is the phosphorylated non-repeating oligosaccharide that links lipid A to the hypervariable O-antigen polymer.[13]

2.3. LPS receptor complex

LPS receptor complex is comprised of LBP (Lipobinding protein), Toll-like receptor 4 (TLR4), MD-2 and CD14**.** CD14 is a myeloid marker antigen.[16] The role of CD14 in LPS activation of monocytes and macrophages has been demonstrated both biochemically and genetically.[17] For example, over expression of human CD14 in transgenic mice renders these mice hypersensitive to LPS, as evidenced by their increased susceptibility to endotoxin shock. In contrast, CD14 deficient mice are hypo-responsive to LPS and are at least 10 times less sensitive to LPS than normal mice.[18] Although CD14 is known to bind LPS it has little signaling capacity because it is bound to the cell membrane by glycosyl phosphatidylinositol (GPI) linkage. MD-2 is a glycoprotein that forms complex with the TLR4. The importance of MD-2 in LPS recognition can be understood by the fact that MD-2 deficient mice exhibit no response to LPS. There is now clear evidence that Toll like receptors (TLRs) mediate the response to LPS.

2.4. Toll-like receptor signaling

Mammalian cells express Toll-like receptors (TLRs) as detectors for variety of molecular patterns on microorganisms.[20] Akira *et al*. studied that families of pattern-recognition receptors detect the microbes which leads to the activation of innate and adaptive immune responses.[22, 23] Toll-like receptors (TLRs) are the best characterized PRRs and are directly responsible for the defense against bacterial and viral infection.[21] After microbial detection, one or more adaptor protein(s) containing a Toll-interleukin 1

(IL-1) receptor (TIR) domain bind(s) to the cytosolic TIR domains of TLRs. Four TIR domain-containing adaptors are involved in propagating TLR signaling: MyD88, TIRAP, TRAM and TRIF. These adaptors link activated TLRs with downstream kinases of the IL-1 receptor associated kinase and mitogen activated protein kinase families, as well as with members of the TRAF family of E3 ubiquitin ligases. Activation of these enzymes leads to the activation of transcriptional regulators such as NF-□B, AP-1 and several interferon-regulatory factors (IRFs), which induce hundreds of genes involved in immune defense.[19] The studies made by Hayashi, F. *et al*. and Toshchakov *et al*. have notified a link between receptor localization, the type of transcriptional response induced and the class of microbe detected.[27, 28] For example, TLR2, TLR4 and TLR5 all recognize different components of bacterial cell wall and, appropriately, are found on the cell surface, where they induce the production of pro-inflammatory cytokines after the detection of microbes.[24,26] In contrast, TLR3, TLR7 and TLR9 detect viral nucleic acids and are found in endolysosomal compartments, where they are poised to detect nucleic acids released after viral degradation.[29, 30, 31] Kagan et al. studied that TLR4 is unique among TLRs. First, TLR4 is the only known TLR able to activate both MyD88-dependent induction of genes encoding inflammatory molecules and TRIF-dependent production of type I interferon.[25] Second, with the exception of TLR4, all other known TLRs are sensors of nucleic acids and induce activation of IRF3 or IRF7 from intracellular compartments. Finally, TLR4 is the only known TLR that engages all four TIR domain-containing adaptors.[32, 33]

2.5. Toll-like receptor 4 (TLR4)

TLR4 mediates lipopolysaccharide signals in collaboration with other molecules, such as CD14, MD-2, myeloid differentiation factor 88 (MyD88) and Toll receptor IL-1 receptor domain containing adapter protein (TIRAP)/MyD88- adapter-like (Mal). TLR4 does not need to heterodimerize with other TLRs to function but forms a complex with several other proteins on the cell surface which are needed for LPS recognition. TLR4 are

often enriched in endosomes after activation. This enrichment leads to increased TLR recognition of PAMPs from phagocytosed pathogens, enhancing activation of TLR signaling pathways and innate immune response.

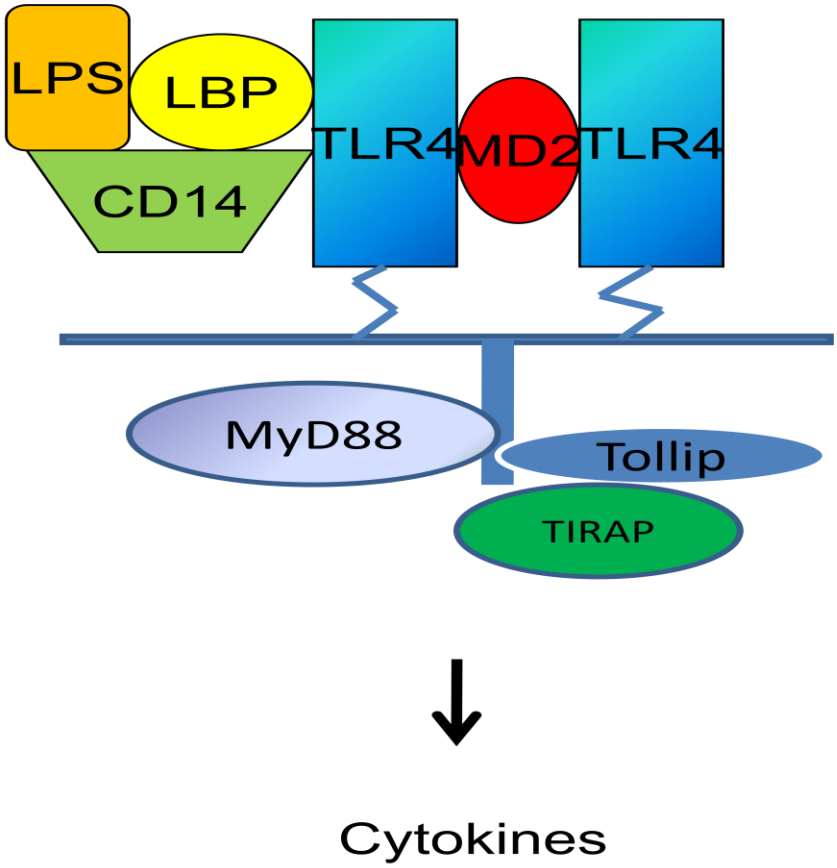

Figure 2. TLR4 signal transduction pathway. LPS binds to the LPS-binding protein (LBP) thereby transferring lipids to CD14. CD14 subsequently transfers LPS to the TLR/MD-2 complexes. TLR4/MD-2 complex transmits signals through MyD88 dependent pathway through Tollip and TIRAP, leading to the secretion of cytokines.

LPS is recognized in mammals by a receptor complex, composed of CD14, TLR4 and MD-2.[35, 36] To elucidate the function of TLR4 Fitzgerald *et al*. constructed chimeric TLR molecules, C-terminally fused to fluorescent proteins and stably expressed these chimerical constructs in cells.[34] These TLR constructs allowed them to study the sub-

cellular localization, dynamics, and ligand interaction of TLRs in the environment of the living cell. Their results demonstrate that:

i. TLR4 is both a surface protein and a Golgi-localized protein.
ii. TLR4 recycles from the surface of cells back and forth to the Golgi.
iii. LPS traffics to the Golgi (this trafficking is not independent of, but occurs together with, its binding receptor; CD-14).[37, 38]
iv. The trafficking of LPS to the Golgi is not necessary for the initiation of cellular activation.

2.6. LPS-monomer or aggregate?

The molecular structure of LPS prepared from R (rough) *Escherichia Coli* $O8^{-}$, SR (semi-rough) Salmonella typhimurium and S (smooth) strains E.coli O8 and Citrobacter 396 are analyzed by Jann *et al* using SDS-PAGE and compared the results from the same LPS preparations by degradation analysis. They showed that in SDS-PAGE, the lipid A content of the different lipopolysaccharide varied and was expressed in their electrophoretic mobilities.[39, 40] Since LPS is heterogeneous and tends to form aggregates of varying sizes, the molecular weight is not very meaningful. The reported range is 2-4 million dalton or greater. When the LPS is treated with SDS and heat, the molecular weight is in the range of 50-100 kDa. In their purest form, in the presence of strong surface active agents, and in the absence of divalent cations, bacterial endotoxins consist of 10-20 kDa macromolecules. In the absence of surface active agents and in the presence of divalent cation sequestering agents such as EDTA, LPS is believed to arrange itself into a micellar structure with a molecular weight of approximately 1,000 kDa. The self aggregation of LPS is generally a function of the lipid A component of the molecule, which also confers the ability to bind to hydrophobic surfaces.

But the active form of LPS, monomer or aggregate, is controversial. Therefore Sasaki *et al*. had examined the aggregation behavior of a nearly homogeneous LPS,

Kdo_2-Lipid A.[41] It is difficult to interpret the immuno-stimulation data using the biophysical multimerization data because the conditions under which cell stimulation experiments are performed are usually different.[42, 43] For instance, critical aggregation concentration in culture medium could be different due to the binding of LPS to serum components such as LBP, sCD14, and lipoproteins.[44,45] Rivera et al. were able to analyze the size heterogeneity of LPS using both gel filtration and SDS-PAGE.[46]

2.7. LPS-TLR4 binding

The mammalian toll-like receptors (TLRs) are germline-encoded receptors expressed by cells of the innate immune system. These receptors are stimulated by structural motifs expressed by bacteria, viruses and fungi known as PAMPs. Importantly, TLR interactions trigger the expression of pro-inflammatory cytokines and help in the functioning of antigen presenting cells of the innate immune system. Many PAMPs have been identified that can stimulate a particular TLRs. For example, the TLR2/TLR6 heterodimer can be stimulated by, lipoteichoic acids (LTA) and peptidolycan (PG). TLR9 is stimulated by viral DNA rich in unmethylated CpG motifs. TLR3 interacts with viral double stranded RNA. Evidences suggests that TLR4 can be stimulated by several PAMPs such as LPS from gram-negative bacteria, fusion (F) protein from respiratory syncytical virus (RSV) and the envelope protein from mouse mammary tumor virus (MMTV).[47] LPS is one of the best studied immune-stimulatory components of bacteria capable to induce systemic inflammation and sepsis if excessive signals occur.[48] Upon LPS recognition TLR4 undergoes oligomerization and recruits downstream adaptors through the interaction with TIR domain.

The relationship between receptor-ligand binding and processing and cellular responses may be explained, at least in part, by determining values of the rate constants for receptor-ligand binding and processing.[52, 53, 54] Shin et al. used the Plasmon Resonance technique to investigate the kinetics involved in the binding of LPS to the recombinant CD14, MD-2 and TLR4 proteins produced in insect cells.[49]

2.8. Fluorescence quenching

At temperature between 0-4 °C, endocytosis is mostly stopped. The use of chemical inhibitors for receptor mediated endocytosis was stated by Nieland *et al.* in their study, where they discovered and characterized small molecules BLT-1, BLT-5 that inhibit the transfer of lipids between HDL and cells mediated by HDL receptor SR-BI.[55] Trypan blue was used to quench surface fluorescence for the flow cytometric assays. Loike et al. were able to demonstrate that trypan blue can quench the fluorescence of glutaraldehyde- fixed red blood cells.[50, 51]

2.9. Flow cytometry

Flow cytometry is a technology that allows a single cell to be measured for a variety of characteristics, determined by looking at how they flow in liquid. Instruments used for this can gather information about cells by measuring visible and fluorescent light emissions, allowing cell sorting based on physical, biochemical and antigenic traits.

When a fluorescently labeled ligand is available its binding to the receptor can be monitored using spectrofluorometry or flow cytometry. Compared to radioligand methods, flow cytometry offers the advantage of monitoring ligand binding to single cells in real-time without the need to separate bound from unbound ligands. Sklar and Finney described that the total number of receptors on the cell membrane can be found by using equilibrium binding assay at 4 °C.[56] Hoffman et al. found that at 4 °C internalization, receptor up-regulation and recycling is minimized, and thus the total number of surface receptors can be assumed constant.[57]

Chapter 3. Experimental Design

3.1. Objective: To establish equilibrium binding constants for LPS interaction with TLR4

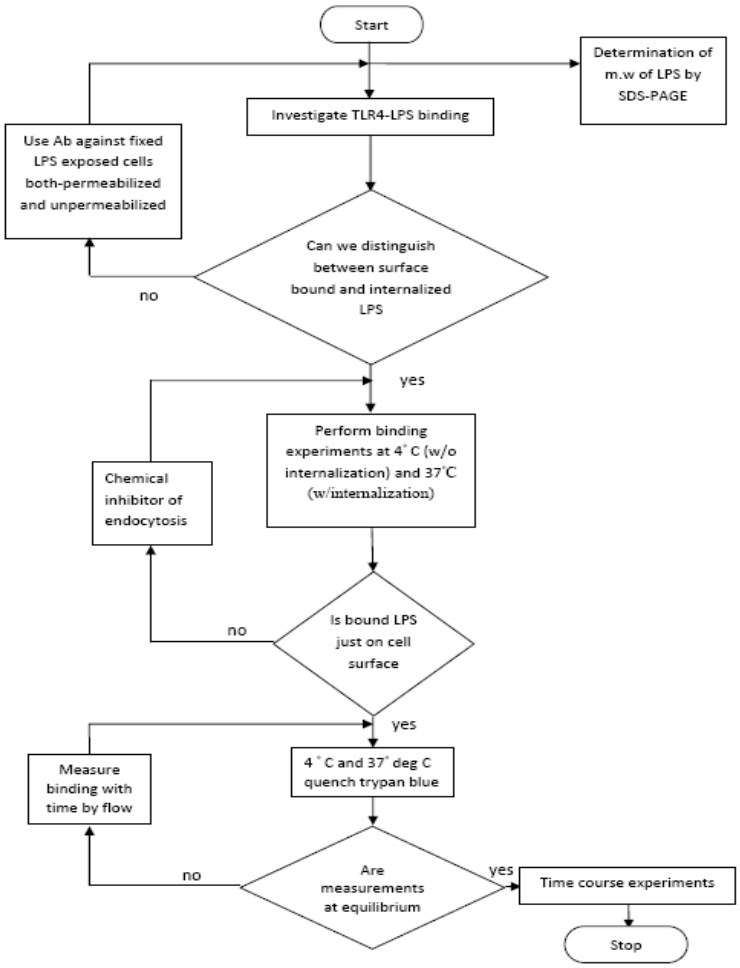

Cell line: IC21 mice macrophage cells were isolated and purified for *in vitro* culture. Cells were grown and maintained at an appropriate temperature and gas mixture (37 C, 5% CO_2 and fetal calf serum) in a cell incubator. Usually it takes 3-4 days for the cells to grow up to 80% confluence. After cells were grown they were separated from the growth medium by centrifugation for 5 minutes at 1200 rpm.

Reagents: Phosphate Buffer Saline (PBS), Trypan Blue, FITC-LPS from Escherichia coli 0111:B4 purchased from Sigma-Aldrich. SDS-PAGE gels were prepared and run using 1x running buffer. 10 ml of 10% separating gel was formed with 4ml of water, 3.3 ml of 30% acrylamide mix, 2.5 ml of 1.5M Tris (pH 8.8), 0.1 ml of 10% SDS, 0.1 ml of 10% ammonium persulfate and 0.004ml of TEMED. 5% stacking gel of 6ml volume if formed with 4.1 ml of water, 1ml of 30% acrylamide mix, 0.75ml of 1.0M Tris (pH 6.8), 0.06 ml of 10% SDS, 0.06ml of 10% ammonium persulfate and 0.006ml of TEMED. Kaleodoscope molecular weight ladder purchased from Biorad.

3.2.1. Determination of LPS molecular weight by using SDS-PAGE

Molecular weight of LPS was determined by using Polyacrylamide gel electrophoresis. Separating gel was poured into the casting setup up to the 4cm mark from the top of the glass plates. The gel was overlaid with water. The gel was allowed to polymerize for 45 minutes. Then, the stacking gel was poured and the comb was inserted with making sure that no air bubbles are formed around the wells. Then the stacking gel was allowed to polymerize for 45 minutes. Then the comb was removed carefully. The formed wells were rinsed several times with water using a squirt bottle and a 100 µl tip**.** The wells were filled with1x running buffer. Three different types of LPS samples are prepared one with PBS, second without PBS, and the last one with PBS and FBS. Duplicate samples were prepared of each kind with each one of the kind sample boiled for 5 minutes. And the rest of the samples remained unboiled. The lower buffer chamber was filled with 1 liter 1x running buffer, and the gel assembly was placed into the lower chamber. Slowly, 500ml of 1x running buffer was poured into a corner of the upper

chamber. The gel was run at 75 volts for 3 hours. The gel is imaged under the scanner using blue light of 50 Å wavelengths under 600 Volts.

3.2.2. Determination of LPS-TLR4 binding at 4 °C

IC21 mice macrophage cells were cultured separated from the growth medium and were counted. The cells were washed twice with PBS and spun in centrifuge at 1250 rpm for 5 minutes. The cells were poured into the wells of 96-well plate at the rate of 20,000 cells per each well. Then cells were stained by the desired concentration of FITC-LPS. The chosen FITC-LPS concentrations are 1, 3, 7, 25, 50 µg/µl. LPS stained cells were placed in an ice bucket for 30 minutes. The 96-well plate was wrapped with aluminum foil to avoid exposure of light. Then, 200 µl of PBS was added to the cells in the wells. Then the samples from each well were transferred into the falcon tubes. The falcon tubes were sent through the FACSAria flow cytometer to measure the fluorescence. The fluorescence intensity of the cells is the direct measure of binding. The experimental results were exported from the flow cytometer in FCS3.0 version (e.g., foo.fcs) following data acquisition.

Flow cytometry data was analyzed using R/Bioconductor.[58] Following installation of R, basic Bioconductor packages and additional packages that are required to process flow cytometry data were downloaded from web within R using:

```
>source ("http://www.bioconductor.org/biocLite.R")

>biocLite("flowCore")

>biocLite("flowViz")

>biocLite("flowUtils")

>biocLite("geneplotter")

>open Vignette()
```

The .fcs files were stored in a new working directory. An array was defined as fclist that contained the data files to be analyzed and were loaded into the R workspace using a single command:

```
> fs <- read.flowSet(fclist, transformation = FALSE)
```

A summary of the loaded flowSet can be shown by typing the variable name at the command line:

```
> fs

A flowSet with 18 experiments.

column names:

FSC-A SSC-A FITC-A Time
```

Gating on cell size

The cell size was gated to exclude non-cellular debris and dead cells which forms non-specific staining. The live cells were separated from the entire cell population by a rectangular gate that selects cells with a certain forward scatter area (e.g. 25000) and maximum intensity (e.g. infinity). Next data driven gate was created that was centered at the median of the specified cell population. The statistics associated with gating were calculated to determine the number of cells retained for subsequent analysis. The live cells were shown in blue using a contour overlay that indicated the density of the cell population.

Linear-Log data Transformation

To eliminate the negative values created after background fluorescent subtraction, the linear values of the fluorescence intensity were transformed into logarithmic values. The relationship used for this transformation was encoded as a function within the script:

```
> linlogTransform = function(transformationId, median = 0, dist = 1, ...)

{tr <- new("transform", .Data = function(x)

{idx = which(x <= median + dist)

idx2 = which(x > median + dist)

if (length(idx2) > 0)

 {x[idx2] = log10(x[idx2] - median) - log10(dist/exp(1))}

if (length(idx) > 0)

 {x[idx] = 1/dist * log10(exp(1)) * (x[idx] - median)}

x})

tr@transformationId = transformationId

tr }
```

Using this transformation function, the background fluorescence obtained from the no stain experiments was subtracted from each of the measured channels. The transition value was held constant for all of the channels at a value of 100. The transforms were applied to the measured fluorescent values. The resulting transformed values were deposited within the flow Frame in a new channel.

3.2.3. Determination of LPS-TLR4 binding at 37 °C

The IC21 cells at 37 °C were exposed to LPS in the similar way as done at 4 °C. But after addition of LPS, cells were incubated in a incubator at 37 °C for 30 minutes. After incubation, the 200 µl of PBS was added to each well of the cells and were transferred into the falcon tubes and fluorescence was measured using flow cytometer.

3.2.4. Fluorescence quenching using Trypan blue

Trypan blue was used to quench the fluorescence on the cell surface membrane. Hence after the cells were exposed to LPS and incubated for half an hour at 4 °C and 37 °C, the cells were added with 200µl of 0.02% trypan blue. The cells at the rate of 20000 cells per each well were incubated with trypan blue for 15 minutes and the fluorescence was measured using flow cytometer.

3.2.5. Determination of LPS-TLR4 binding with respect to time

Binding of LPS to TLR4 with time at 37 °C was found by adding FITC-LPS to the IC 21 mice cells at different intervals of time, up to 3 hours. Fluorescence of cells was measured at different time points. The obtained data was analyzed by using R, to determine the equilibrium binding time.

3.2.6. Determination of Dissociation Constant

The Dissociation constant, k_D, was determined using binding assay at 4 °C After subtraction of background fluorescence from the total fluorescence obtained for each ligand concentration, the concentration of free ligand and receptor-ligand complexes was determined. The total number of surface TLR4 receptor, R_{tot} and the apparent equilibrium dissociation constant k_D were evaluated by minimizing the squared residual of the data points in a fit to a one site model.

As a base model of receptor-ligand binding, monovalent ligand model was considered where ligand, L, binds reversibly to a monovalent receptor, R, to form a receptor-ligand complex, C;

$$R + L \Leftrightarrow C \tag{1}$$

The the time rate change of the concentration of receptor-ligand complex as a function of the free receptor number R and the ligand concentration L , where k_f (M^{-1} sec^{-1}) is the association rate constant while k_r (sec^{-1}) is the dissociation rate constant is described by:

$$\frac{dC}{dt} = k_f[R][L] - k_r[C] \quad (2)$$

To solve equation (2) a situation is to be considered where the total number of surface receptors remains unchanged. In addition, the ligand concentration remains constant irrespective of receptor binding. Therefore

$$R_{tot} = R + C \quad (3)$$

Hence,

$$\frac{dC}{dt} = k_f[R_{tot} - C]L - k_rC \quad (4)$$

The number of receptor-ligand complexes at equilibrium, C_{eq} at steady state i.e. dC/dt =0 is;

$$C_{eq} = \frac{R_{tot}L}{k_D+L} \quad (5)$$

Where k_D, the equilibrium dissociation constant, is equal to k_r/k_f.

The ligand can also interact with the cell in a non-specific manner. Non-specific binding is proportional to the ligand concentration:

$$C_{NS} = K_{NS} * L \quad (6)$$

Where C_{NS} is the concentration of non-specifically bound ligand and K_{NS} is a nonspecific proportionality constant expressed in terms of $\frac{sites}{cell} * \frac{volume}{moles}$. Ligand bound to the cell is the sum of specific and non-specific binding:

$$C_{tot} = C_{eq} + C_{NS} \tag{7}$$

$$C_{tot} = \frac{R_{tot}\, L}{K_D + L} + K_{NS} * L \tag{8}$$

Therefore, the two terms in the R.H.S of the equation # 8 represent specific and non-specific binding respectively.

Now, the equation # 8 was used to determine the constants Rtot, KD and KNS. As, the fluorescence intensity measure of the cells obtained was the result of both specific and non-specific binding of the ligand, fluorescence intensity was calculated by making suitable assumptions and many iterations were made until the error between experimentally obtained fluorescent measure and theoretically obtained fluorescent measure was minimized. The calculations were done in excel sheets.

3.3. Results

3.3.1. Lipopolysaccharide (LPS) analysis by SDS-PAGE

An applied electric field across the gel caused the negatively charged sample molecules to migrate across the gel towards the anode. Depending upon the size, the molecules moved differently through the gel: low-molecular-weight molecules moving more easily than the high-molecular-weight ones. The gel is calibrated by running the kaleidoscope molecular-weight marker in the separate lane. The scanned image of the gel is obtained and molecular weight of the FITC-LPS samples in the gel is determined by comparing the distance travelled by the sample relative to the molecular-weight marker. Figure 1 shows the scanned image of the FITC-LPS samples in the polyacrylamide being compared with the molecular weight marker.

As we see from the figure the image of the FITC-LPS sample in the presence of FBS has high-molecular-weight than the other two FITC-LPS samples. This may be attributed to the fact that FBS contains lipoproteins which adhered to LPS molecules, thereby increasing the size of the molecule. The other two samples did not differ much in their size indicating that boiling had a minimal effect on the molecular weight of the LPS samples before running through the gel. The image of the high concentration LPS samples was darker than the low concentration LPS samples.

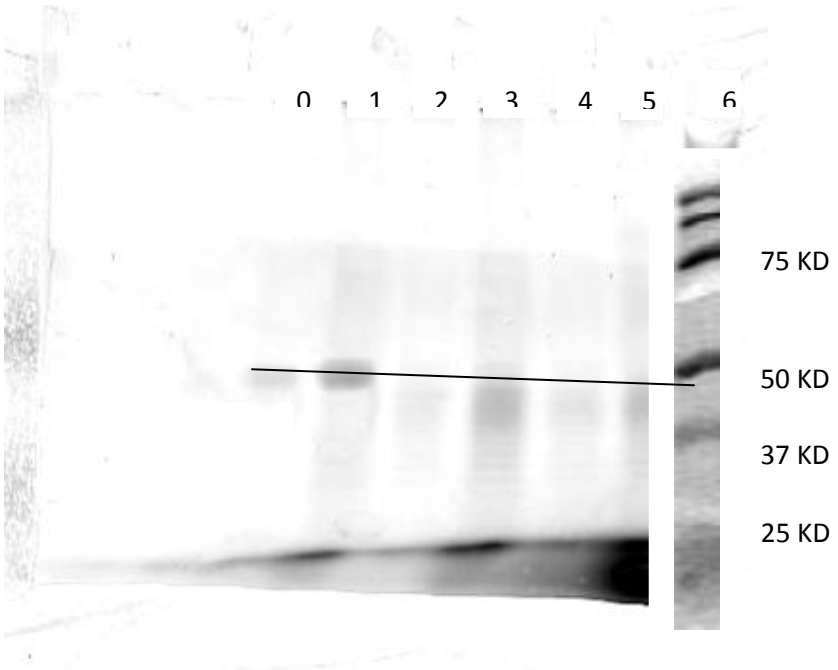

Figure 3. Scanned image of LPS samples in SDS-PAGE. Wells formed in stacking gel were numbered from 6 to 0. In the well 6, Molecular weight marker was filled. In wells 5 and 4, 5µg and 1µg boiled LPS samples in presence of PBS was added. In wells 3 and 2, 5 µg and 1µg LPS samples in presence of PBS was added. In wells 1 and 0, LPS 5µg and 1µg LPS samples in presence of FBS and PBS was added.

A

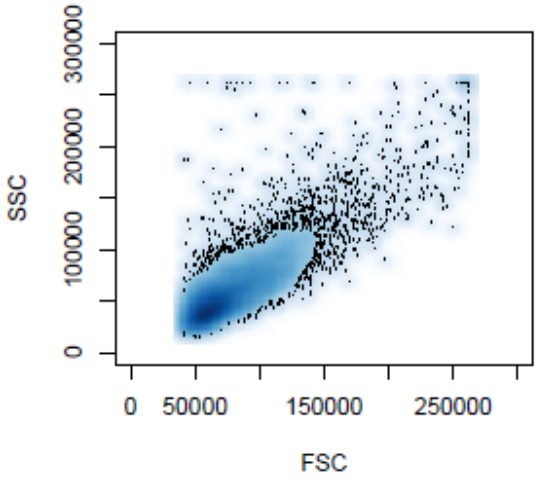
SSC
0
100000
200000
300000
0
50000
150000
250000
FSC

B

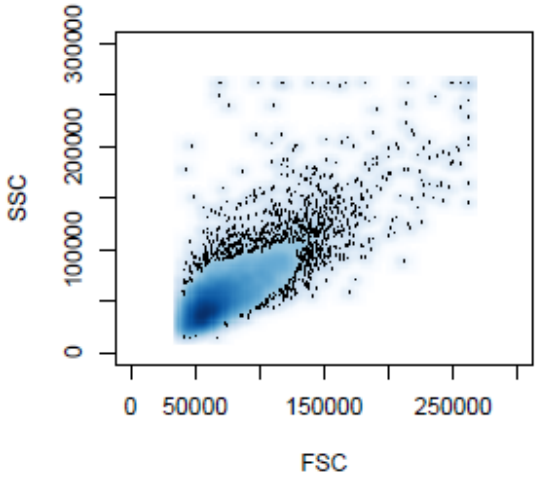
SSC
0
100000
200000
300000
0
50000
150000
250000
FSC

C

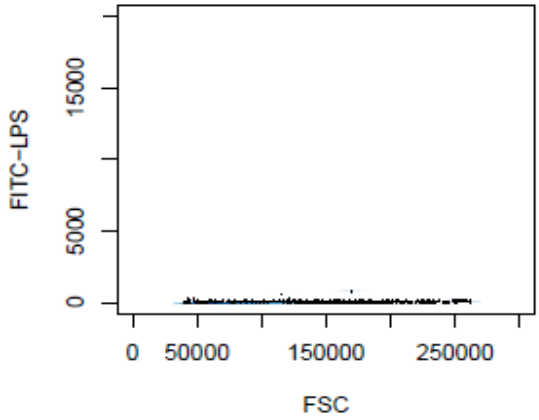
FITC-LPS
0
5000
15000
0
50000
150000
250000
FSC

D

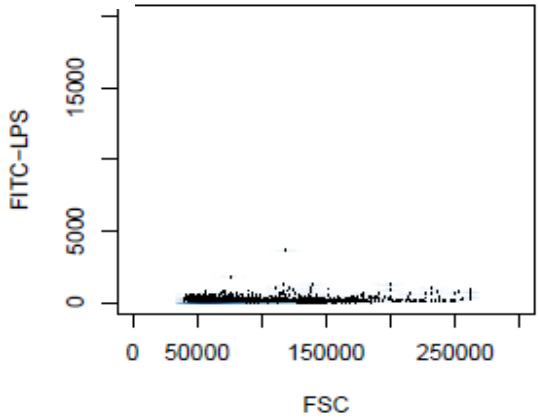
FITC-LPS
0
5000
15000
0
50000
150000
250000
FSC

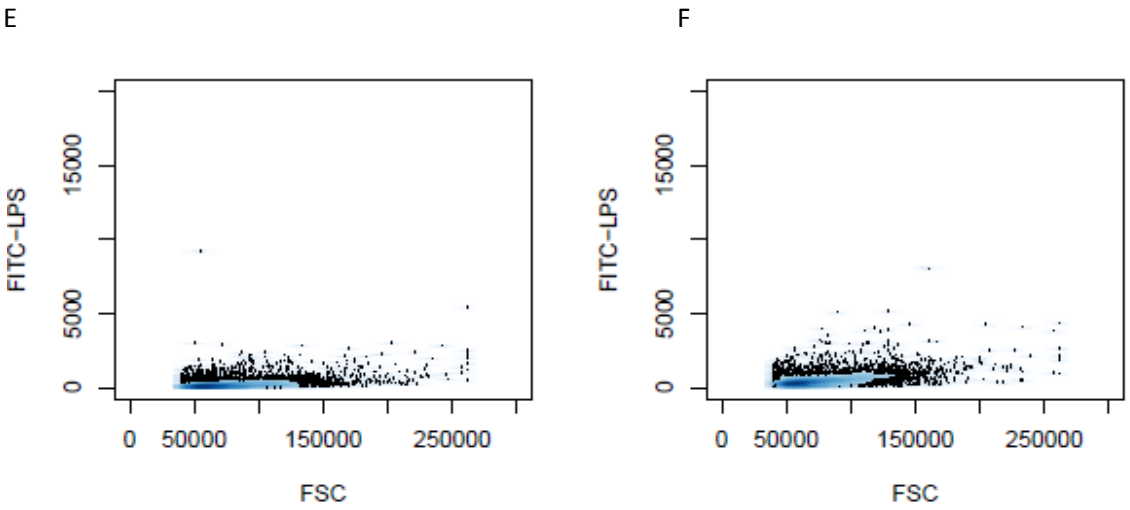

Figure 4. Forward Scatter-Side Scatter plots for LPS-TLR4 binding at 4 °C. The dots scattered outside the contour are the cells rejected. Plot A represents the FSC-SSC for unstained IC21 mice cells at 4 °C, B for cells stained with 1 µg/ml LPS, C represents plot of concentration of LPS versus FSC for unstained cell, D represents plot of log of concentration of LPS versus FSC for cells stained with 1 µg/ml LPS, E and F represents the plots of concentration of LPS versus FSC for 3 and 7 µg/ml respectively.

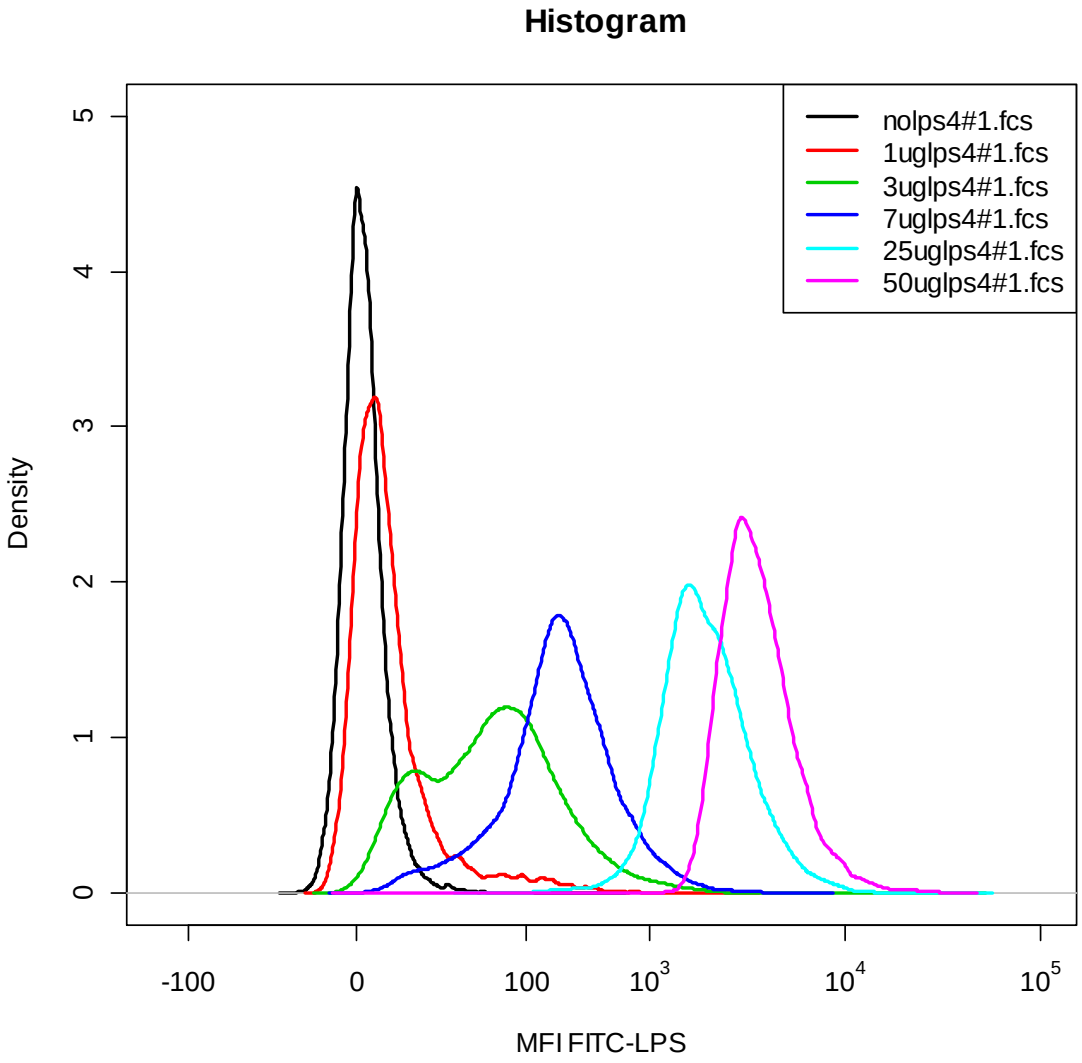

Figure 5. Histogram of LPS-TLR4 binding at 4 °C. The area under each curve represents the population density exhibiting fluorescence measured along horizontal axis. Black curve represents the background fluorescence exhibited by unstained cells at 4 °C, red, green, violet, blue and pink curves represents the fluorescence exhibited by the IC21 mice cells stained with 1, 3,7,25,50 µg/ml LPS respectively.

Table 1. Cell viability data for LPS-TLR4 binding at 4 °C

Dose	total cells	#events	live cells	percentage	LPS+	MFI
No lps	10000	10000	9773	97.3	55	22
1ug lps	10000	10000	9738	97.3	132	28
3ug lps	10000	10000	9746	97.4	396	35
7ug lps	10000	10000	9762	97.6	9153	204
25ug lps	10000	10000	9630	96.3	9604	1238
50ug lps	10000	10000	9584	95.8	9573	1670

3.3.2. Determination of LPS-TLR4 binding at 4 °C

At 4 °C, receptor trafficking, endocytosis and pinocytosis are stopped. Therefore it becomes easy to quantitate the ligand receptor binding in terms of equilibrium binding constant. The FSC-SSC plots for LPS-TLR4 binding at 4 °C are shown in Figure 4. FSC correlates with the cell volume and SSC depends on the inner complexity of the particle. Hence these plots show fluorescent molecules bound to the cell. The histogram in Figure 5, shows the density distribution of the cells expressing fluorescence for increasing amount of ligand concentration.

The fluorescence intensity was quenched by using trypan blue[58]. Figure 7 shows the fluorescence quenching obtained at 4 °C. The surface fluorescence was quenched by trypan blue, and the remaining fluorescence which we can see was due to the internalized LPS or nonspecific binding. The amount of fluorescence quenched at 37 °C was much lower than that of quenched at 4 °C. Any fluorescence of quenched samples, which we see for the cells stained with high concentration of LPS, may be due to the inadequate amount of the trypan blue.

Figure 7 shows the fluorescence quenching of the cells obtained at 4 °C. The fluorescence of all the samples, after addition of trypan blue was close to the background fluorescence of unstained cells. From which, it becomes clear that at 4 °C receptor mediated endocytosis, pinocytosis and internalization processes are negligible.

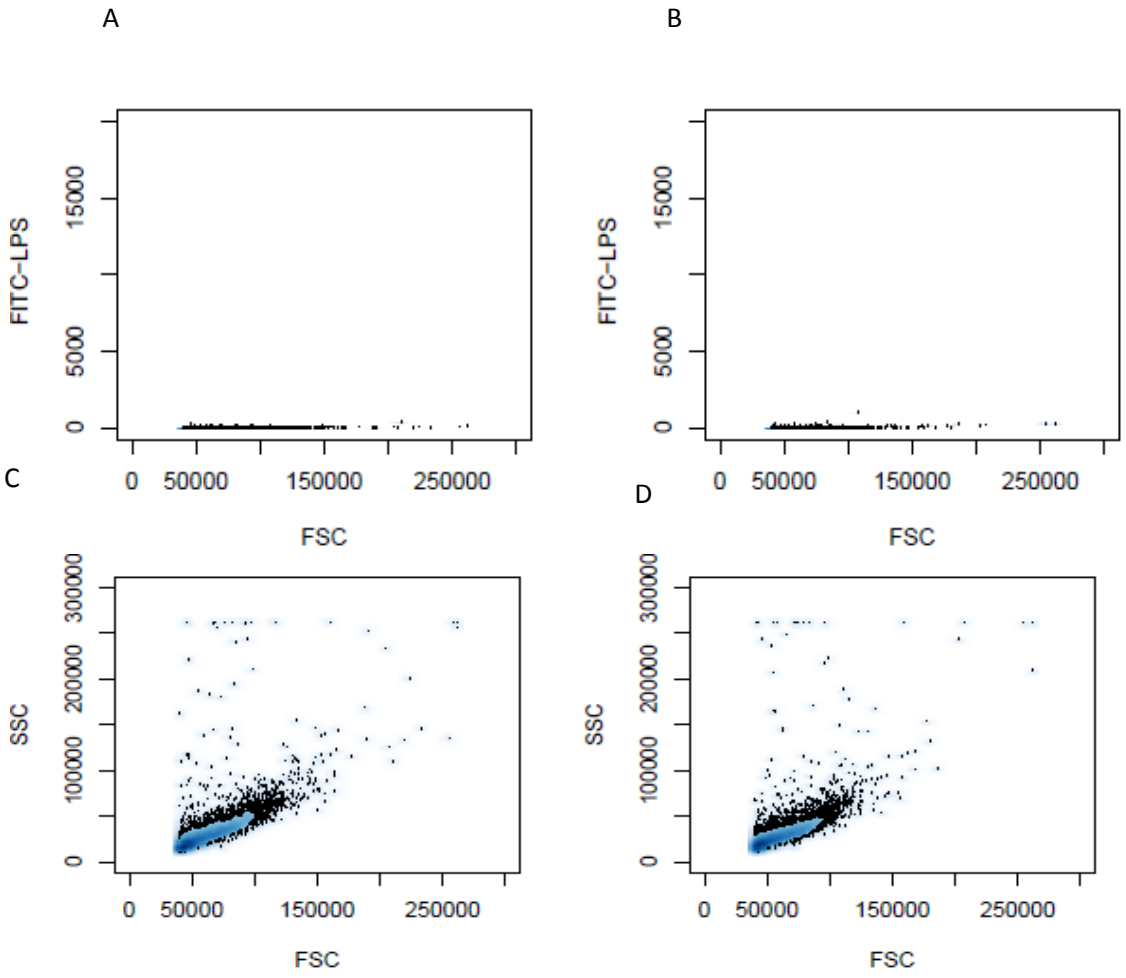

Figure 6. Forward Scatter- Side Scatter plots for fluorescence quenching at 4 °C. The dots scattered outside the contour are the cells rejected. Plot A represents the FSC-SSC for unstained IC21 mice cells quenched with trypan blue at 4 °C, B for cells stained with 1 µg/ml LPS, quenched with trypan blue, C represents plot of concentration of LPS versus FSC for unstained cell, quenched with trypan blue, D represents plot of log of concentration of LPS versus FSC for cells stained with 1 µg/ml LPS, quenched with trypan blue.

A

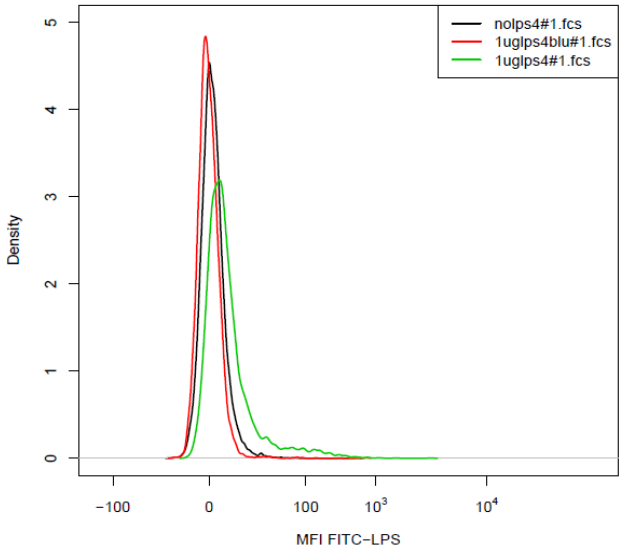
nolps4#1.fcs
1uglps4blu#1.fcs
1uglps4#1.fcs
Density
MFI FITC−LPS

B

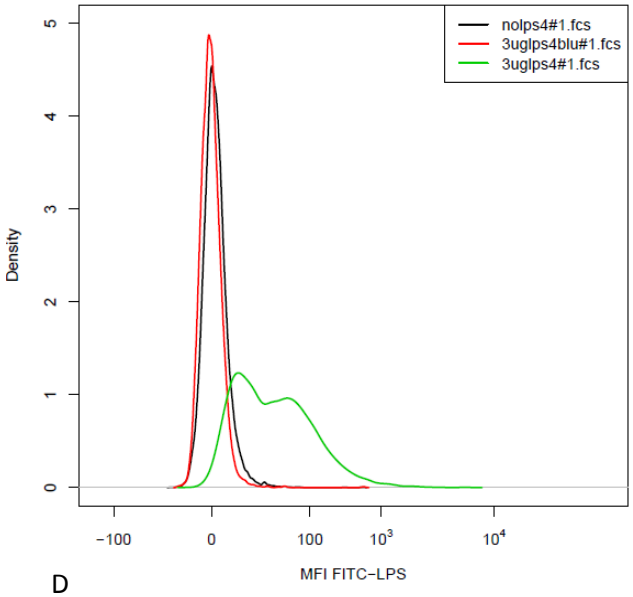
nolps4#1.fcs
3uglps4blu#1.fcs
3uglps4#1.fcs
Density
MFI FITC−LPS

C

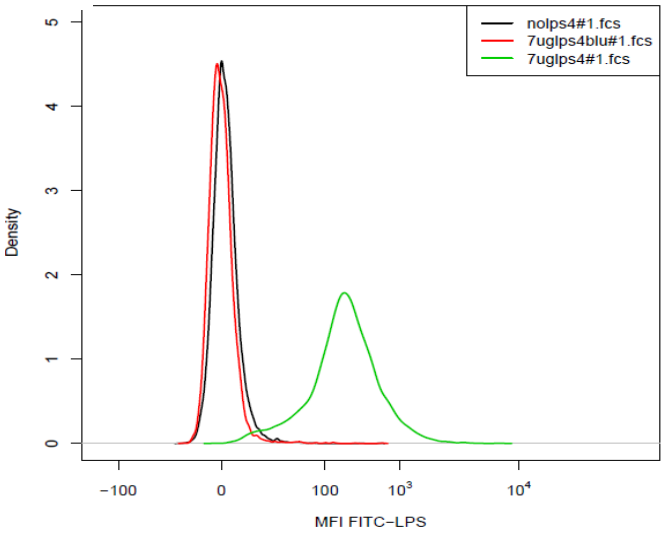
nolps4#1.fcs
7uglps4blu#1.fcs
7uglps4#1.fcs
Density
MFI FITC−LPS

D

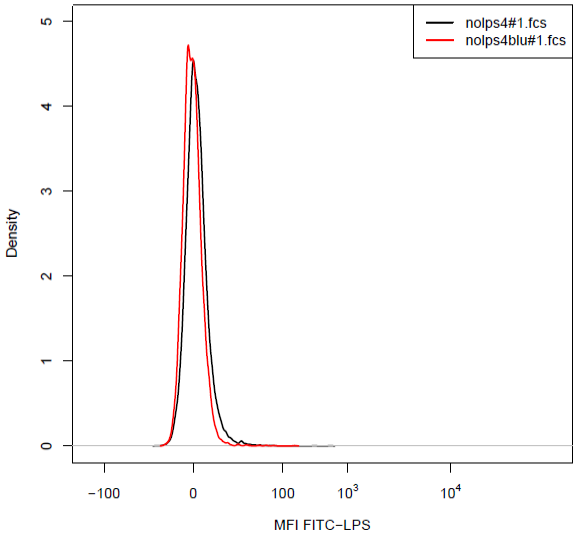
nolps4#1.fcs
nolps4blu#1.fcs
Density
MFI FITC−LPS

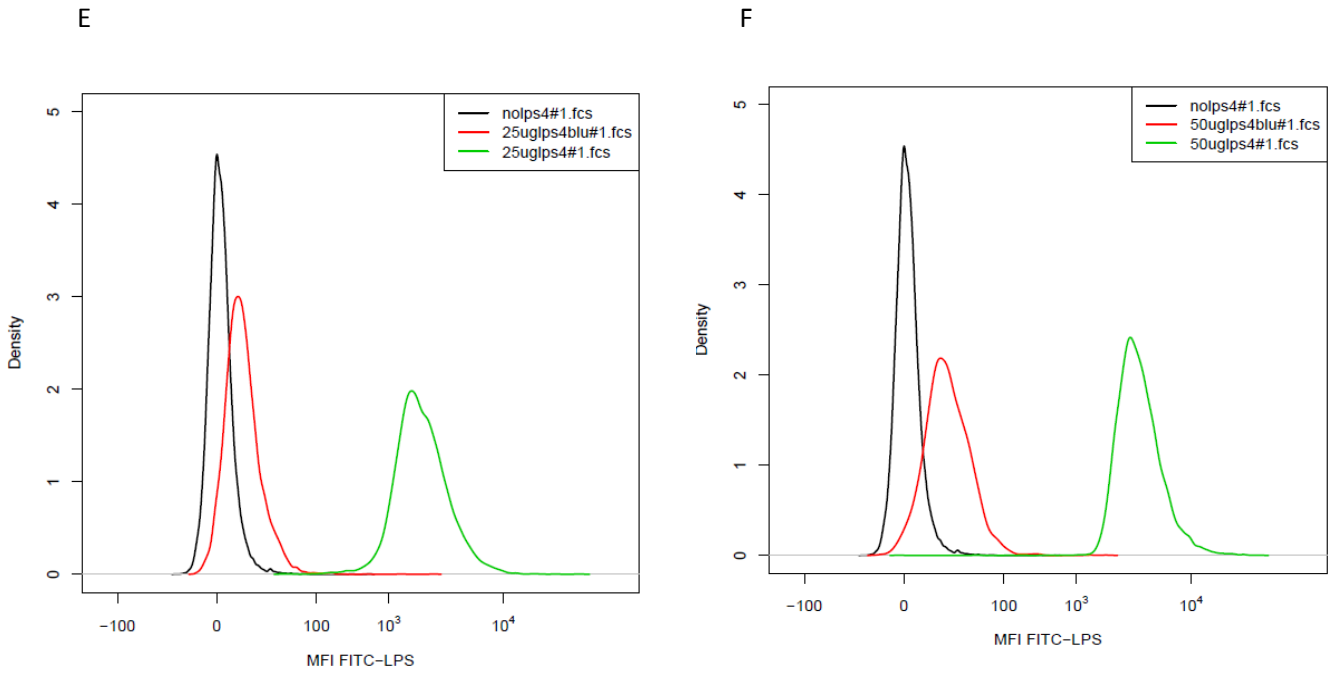

Figure 7. Histogram of fluorescence quenching by trypan blue obtained at 4 °C. Each subpanel has three curves, one representing background fluorescence, and other two representing density distribution of fluorescence intensity obtained with and without addition of trypan blue for different ligand concentrations. A represents the density distribution curves of unstained cells with and without addition of trypan blue. B, C, D, E and F represents the density distribution curves for cells stained 1, 3, 7, 25 and 50 µg/ml ligand concentration, with and without addition of trypan blue. We can see that fluorescence expressed by cells for 1, 3, 7 µM concentration of FITC-LPS was almost equal to the background fluorescence. At higher ligand concentration, fluorescence was partially quenched.

Table 2. Cell viability data for Fluorescence quenching of LPS at 4 °C

Dose	**Total cells**	**Live cells**	**Percentage**	**LPS+**	**MFI**
no lps	10000	9741	97.4	11	11
1ug lps	10000	9695	96.9	15	12
3ug lps	10000	9687	96.8	18	13
7ug lps	10000	9639	96.4	22	11
25ug lps	10000	9689	96.9	898	56
50ug lps	10000	9456	94.6	1916	65

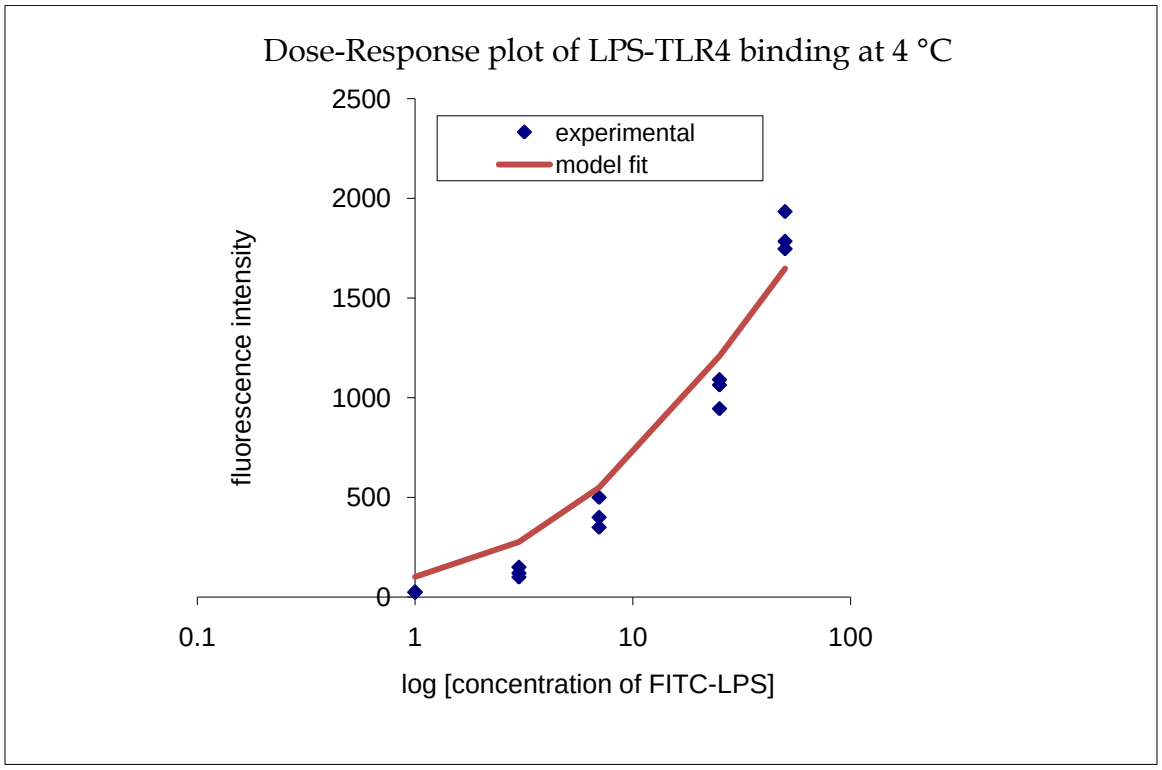

Figure 8. Dose-Responses plot of LPS-TLR4 binding at 4 °C. Experimental dose response corresponds to the fluorescent intensity measured by flow cytometer, model fit curve is obtained by simulation, using equation 8, mentioned in materials and methods section.The dissociation constant K_D obtained from the kinetics plots was 16.0 µM, Rtot or maximum intensity obtained was 1800, and K_{ns}, non-specific binding constant was calculated to be 6.5 μM^{-1}(assuming, single binding site for each cell).

3.3.3. Determination of LPS-TLR4 binding at 37 °C

At 37 °C receptor synthesis, degradation, and trafficking occurs through the cell membrane. Ligand/Receptor complexes traffic through the cell membrane into the cell. The FSC-SSC plots for LPS-TLR4 binding at 37 °C are shown in Figure 9. We can see that fluorescence intensity was increased relating to the results obtained at 4 °C under similar experimental conditions, from Figure 10. This was because of internalization of ligand or ligand/receptor complex inside the cell. The LPS concentrations of 1, 3, 5, 7,

25, 50 µM were added to the cells at 37 °C. Figure 8 shows the dose response of the cells. The fluorescence intensity continuously increased with the increase in concentration of the ligand added. Trypan blue was added to determine the internalized LPS at 37 °C. Trypan blue quenched the fluorescence obtained at 37 °C, but was comparatively less than that quenched at 4 °C. Figure 12, shows the histogram of population distribution expressing fluorescence after the addition of trypan blue at 37 °C.

Figure 13 shows the dose response plot of the flow cytometry data for experiments with and without addition of trypan blue at 4 °C and 37 °C.

A

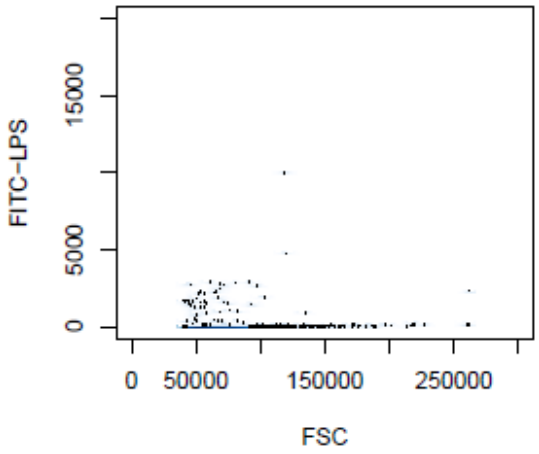
FITC-LPS
15000
5000
0
0
50000
150000
250000
FSC

B

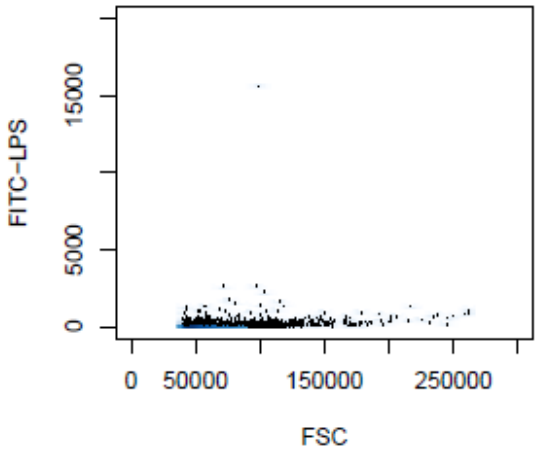
FITC-LPS
15000
5000
0
0
50000
150000
250000
FSC

C

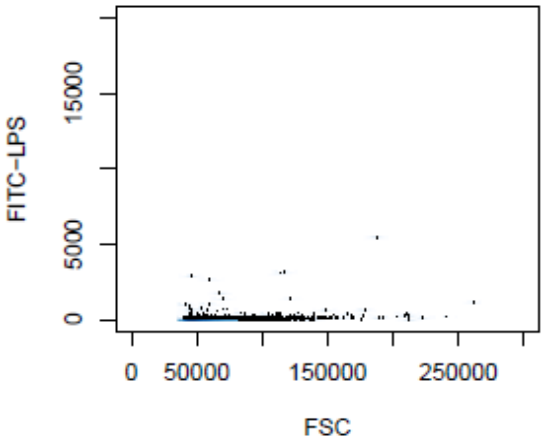
FITC-LPS
15000
5000
0
0
50000
150000
250000
FSC

D

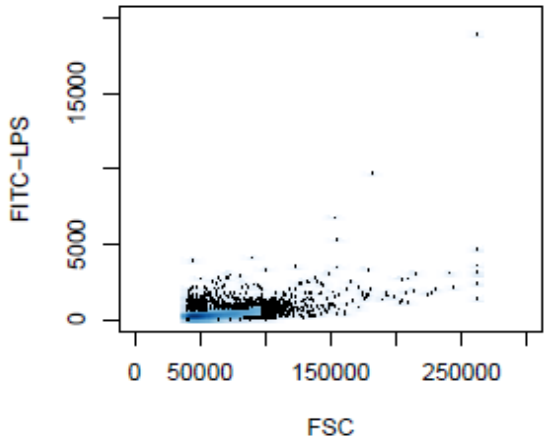
FITC-LPS
15000
5000
0
0
50000
150000
250000
FSC

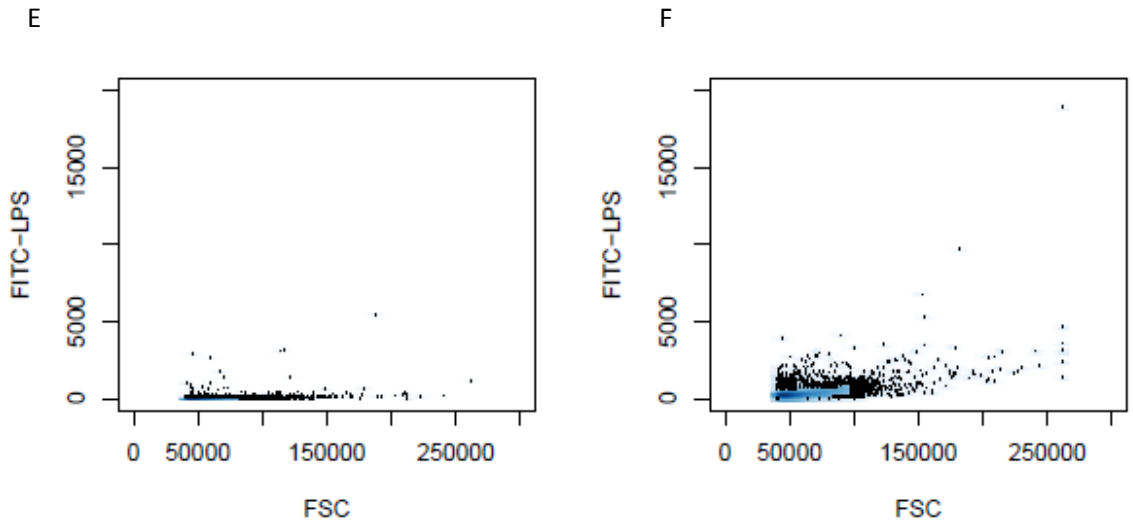

Figure 9. Forward Scatter-Side Scatter plots for LPS-TLR4 binding at 37 °C. The dots scattered outside the contour are the cells rejected. Plot A represents the FSC-SSC for unstained IC21 mice cells at 37 °C, B for cells stained with 1 µg/ml LPS, C represents plot of concentration of LPS versus FSC for unstained cell, D represents plot of log of concentration of LPS versus FSC for cells stained with 1 µg/ml LPS, E and F represents the plots of concentration of LPS versus FSC for 3 and 7 µg/ml respectively.

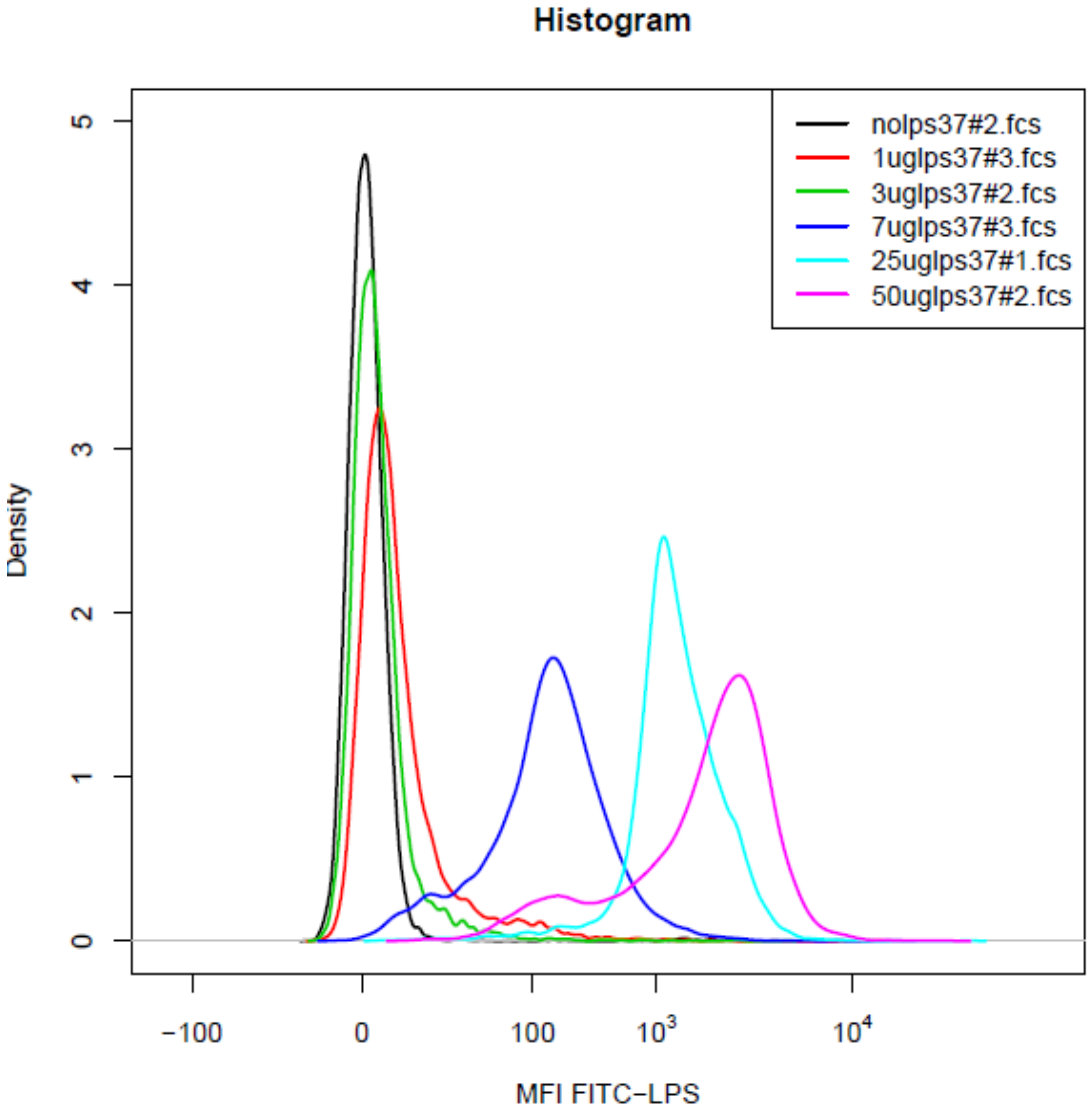

Figure 10. Histogram of LPS-TLR4 binding at 37 °C. The area under each curve represents the population density exhibiting fluorescence measured along horizontal axis. The black curve represents the fluorescence exhibited by unstained cells or background fluorescence, and the remaining curves represent the dose response, which increased with increase in the concentration of FITC-LPS.

Table 3. Cell viability data for LPS-TLR4 binding at 37 °C

Dose	total cells	live cells	percentage	LPS+	MFI
No lps	10000	9773	97.7	55	27
1ug lps	10000	9738	97.4	132	62
3ug lps	10000	9746	97.5	396	154
7ug lps	10000	9762	97.6	9153	410
25ug lps	10000	9630	96.3	9604	1645
50ug lps	10000	9584	95.84	9573	2470

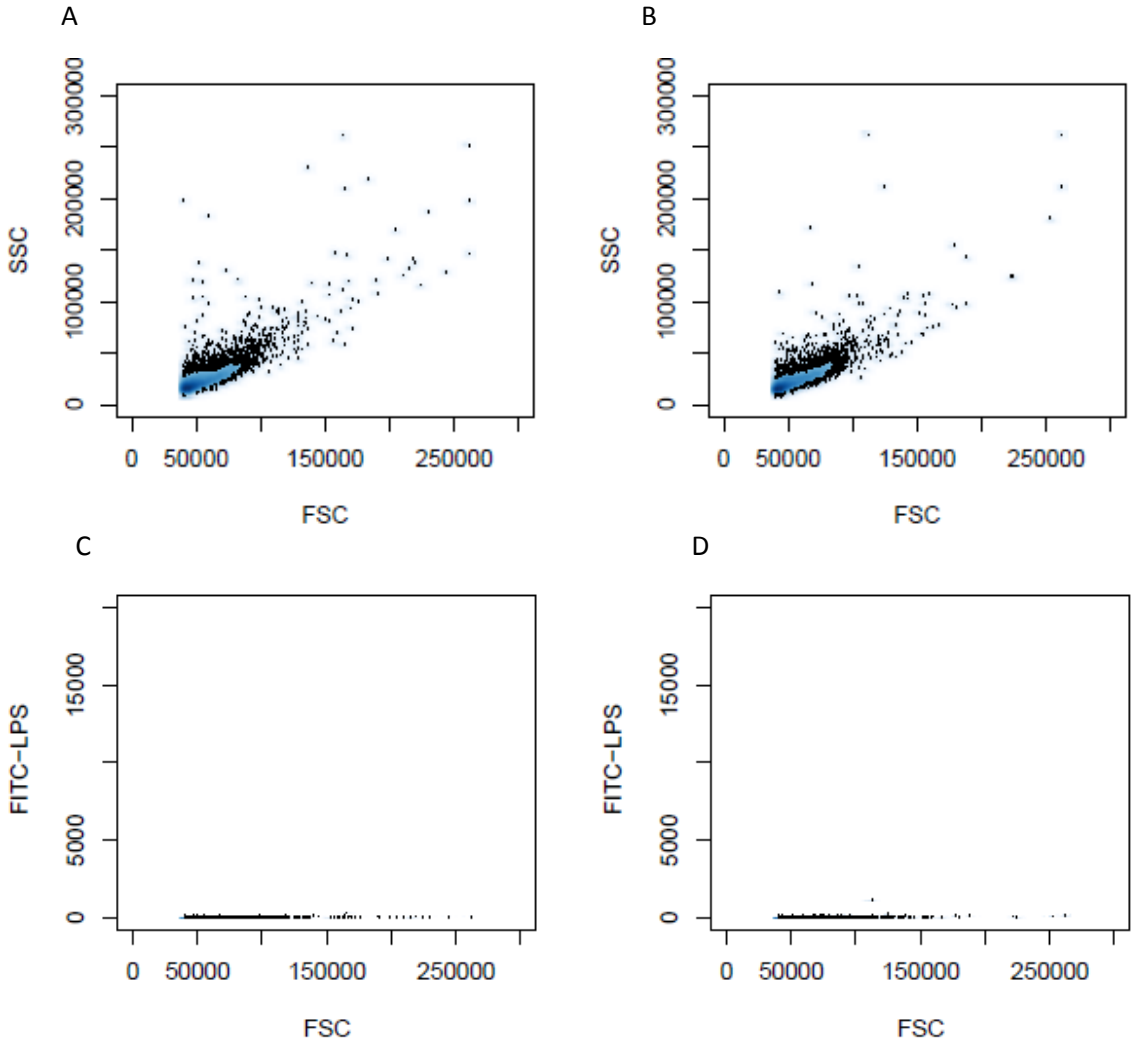

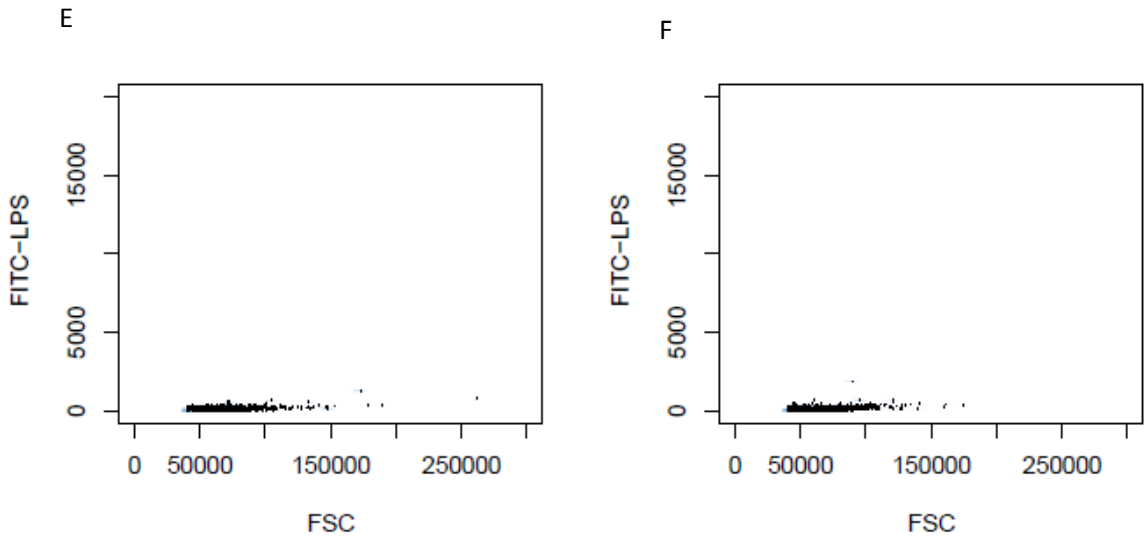

Figure 11. Forward Scatter-Side Scatter plots for fluorescence quenching at 37 °C. The dots scattered outside the contour are the cells rejected. Plot A represents the FSC-SSC for unstained IC21 mice cells quenched with trypan blue at 4 °C, B for cells stained with 1 µg/ml LPS, quenched with trypan blue, C represents plot of concentration of LPS versus FSC for unstained cell, quenched with trypan blue, D represents plot of log of concentration of LPS versus FSC for cells stained with 1 µg/ml LPS, quenched with trypan blue.

A

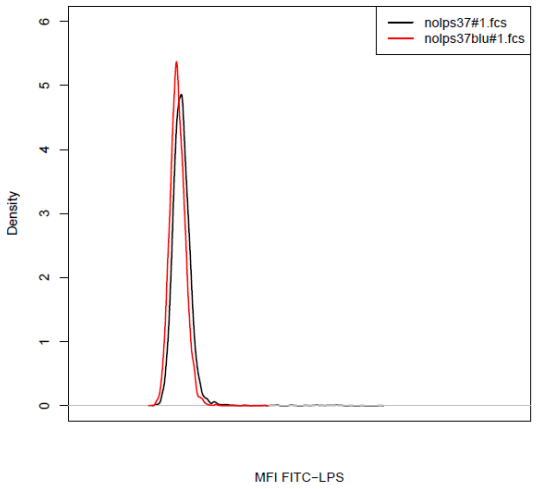
nolps37#1.fcs
nolps37blu#1.fcs
Density
MFI FITC-LPS

B

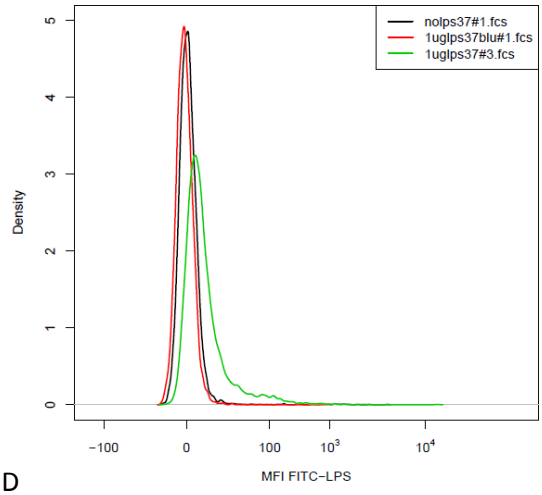
nolps37#1.fcs
1uglps37blu#1.fcs
1uglps37#3.fcs
Density
MFI FITC-LPS

C

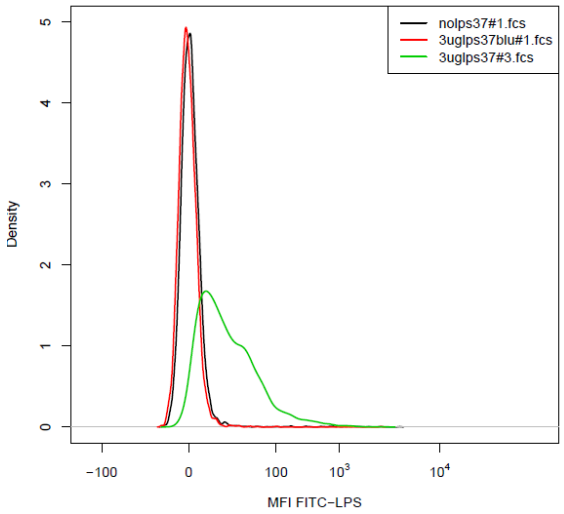
nolps37#1.fcs
3uglps37blu#1.fcs
3uglps37#3.fcs
Density
MFI FITC-LPS

D

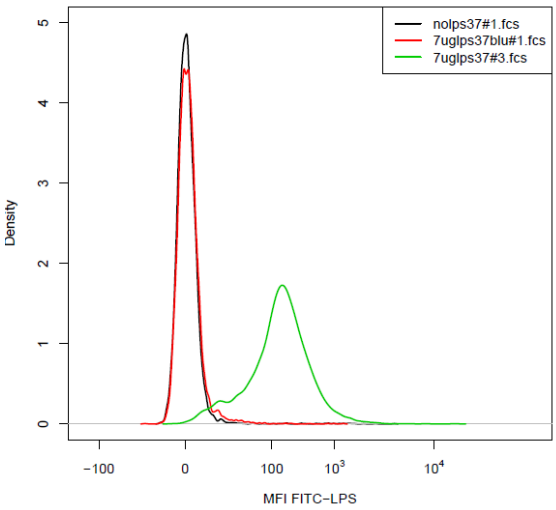
nolps37#1.fcs
7uglps37blu#1.fcs
7uglps37#3.fcs
Density
MFI FITC-LPS

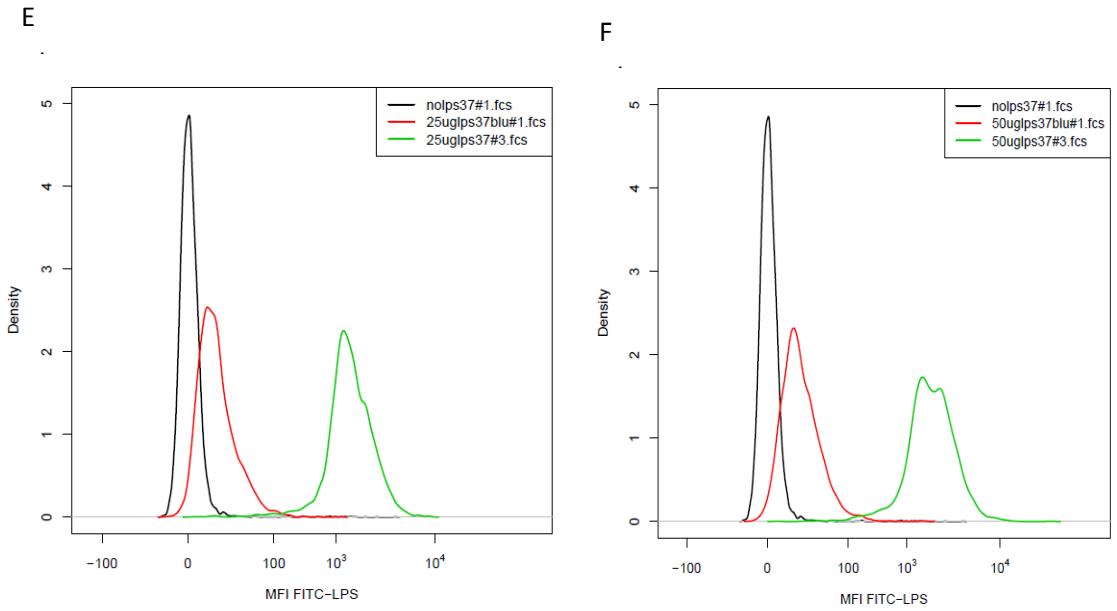

Figure 12. Histogram of Fluorescence quenching at 37 °C. Each subpanel has three curves, one representing background fluorescence, and other two representing density distribution of fluorescence intensity obtained with and without addition of trypan blue for different ligand concentrations. A represents the density distribution curves of unstained cells with and without addition of trypan blue. B, C, D, E and F represents the density distribution curves for cells stained 1, 3, 7, 25 and 50 µg/ml ligand concentration, with and without addition of trypan blue. We can see that fluorescence expressed by cells for 1, 3, 7 µM concentration of FITC-LPS was almost equal to the background fluorescence. At higher ligand concentration, fluorescence was partially quenched. We can see that fluorescence expressed by cells for 1, 3, 7 µM concentration of FITC-LPS was almost equal to the background fluorescence. At higher ligand concentration, fluorescence was partially quenched.

Table 4. Cell viability data for fluorescence quenching at 37 °C

Dose	**Total cells**	**Live cells**	**Percentage**	**LPS+**	**MFI**
no lps	10000	9777	97.8	6	7
1ug lps	10000	9818	98.2	8	8
3ug lps	10000	9828	98.3	19	10
7ug lps	10000	9756	97.6	110	19
25ug lps	10000	9461	94.5	1320	65
50ug lps	10000	9383	93.8	2628	83

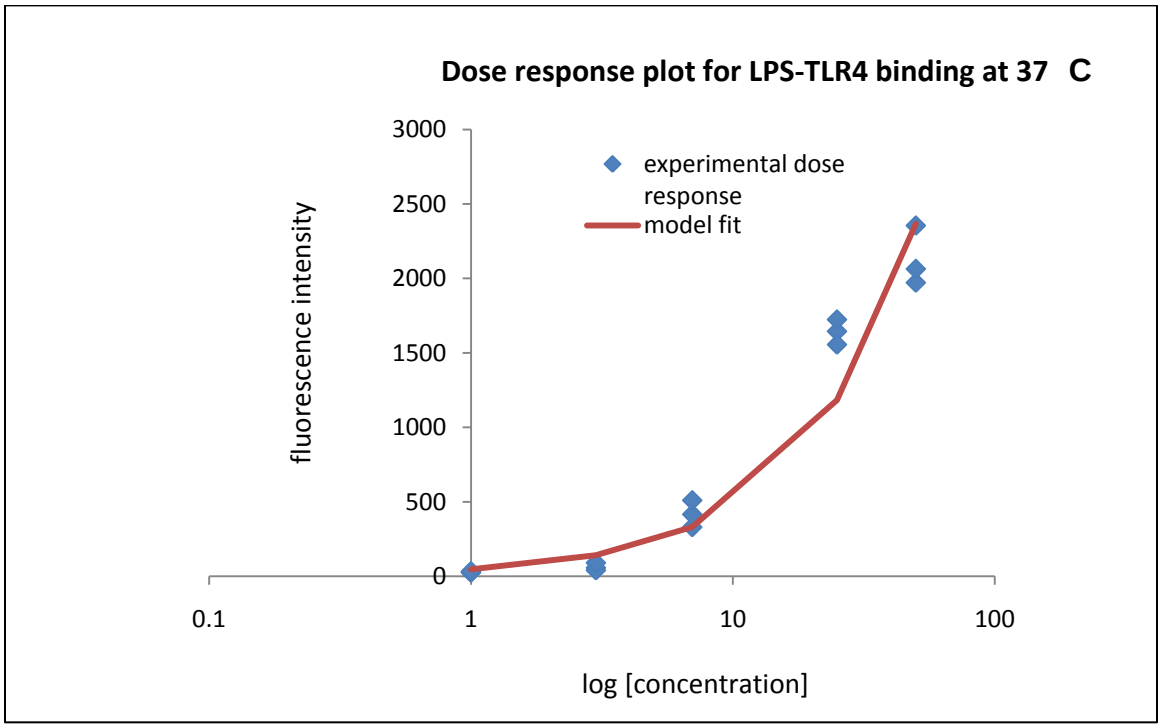

Figure 13. Dose response plot of LPS-TLR4 binding at 37 °C. Experimental dose response corresponds to the fluorescent intensity measured by flow cytometer, model fit curve is obtained by simulation, using equation 8, mentioned in materials and methods section. The dissociation constant K_D obtained from the kinetics plots was 56.30 µM, Rtot or maximum intensity obtained was 2500, and K_{ns}, non-specific binding constant was calculated to be 1.92 μM^{-1}(assuming, single binding site for each cell).

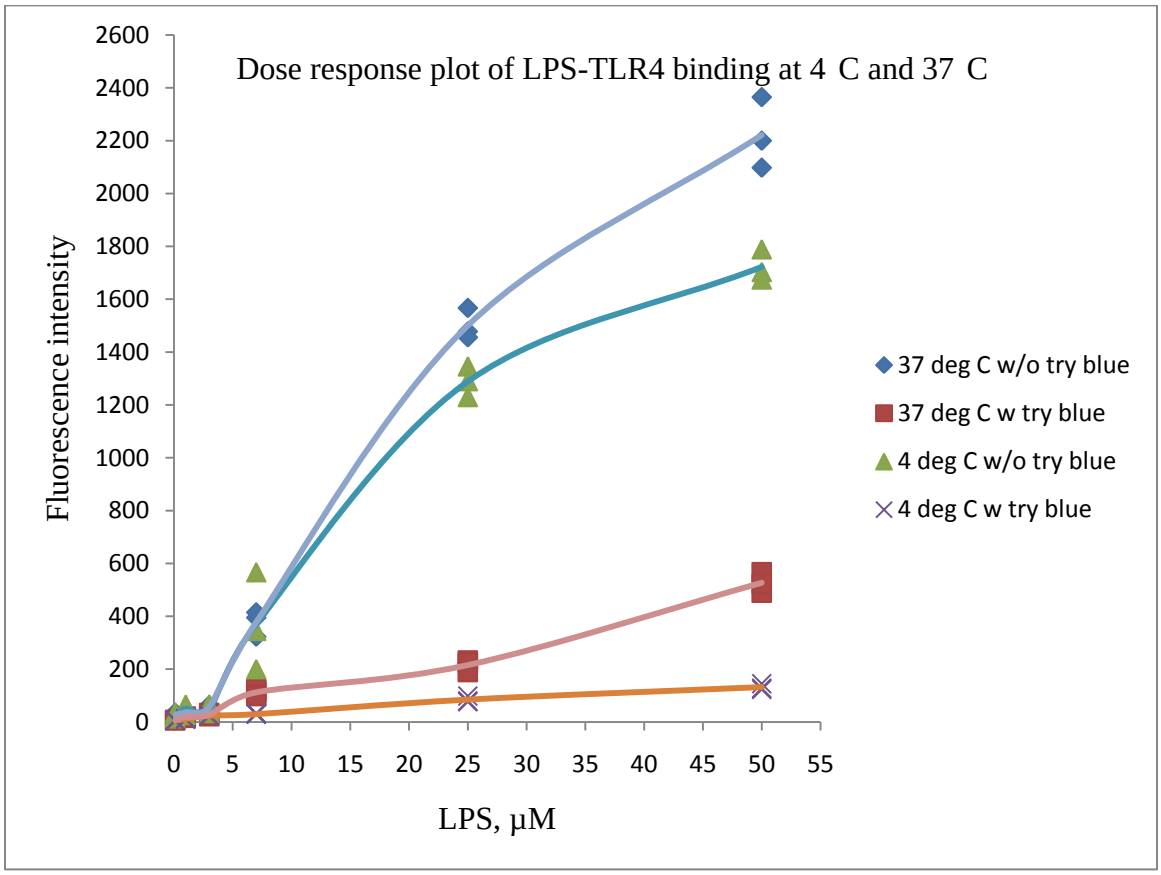

Figure 14. Dose response plot of LPS –TLR4 binding +/- Tryplan blue at 4 °C and 37 °C. The fluorescence intensity expressed by the cells at 4 °C was almost quenched by trypan blue, whereas at 37 °C, it was partially quenched.

3.3.5. Study of LPS-TLR4 binding with respect to time

LPS binding with respect to time was studied to determine the equilibrium binding. Time-course experiments were carried out at 5 different time points with 2 different concentration 1, 7 µg/µl of LPS. Figure 13 shows the histogram of LPS-TLR4 binding at different time points at 37 °C. Figure 14 shows the histogram of fluorescence quenching obtained for time course experiments. Figure 15 shows the plot of the dose response of the LPS-TLR4 binding with respect to time. From Figure 14, we can see the gradual increase of fluorescence intensity with respect to time upto 30 minutes for all the samples. Therefore the equilibrium binding was supposed to take place at 30 minutes.

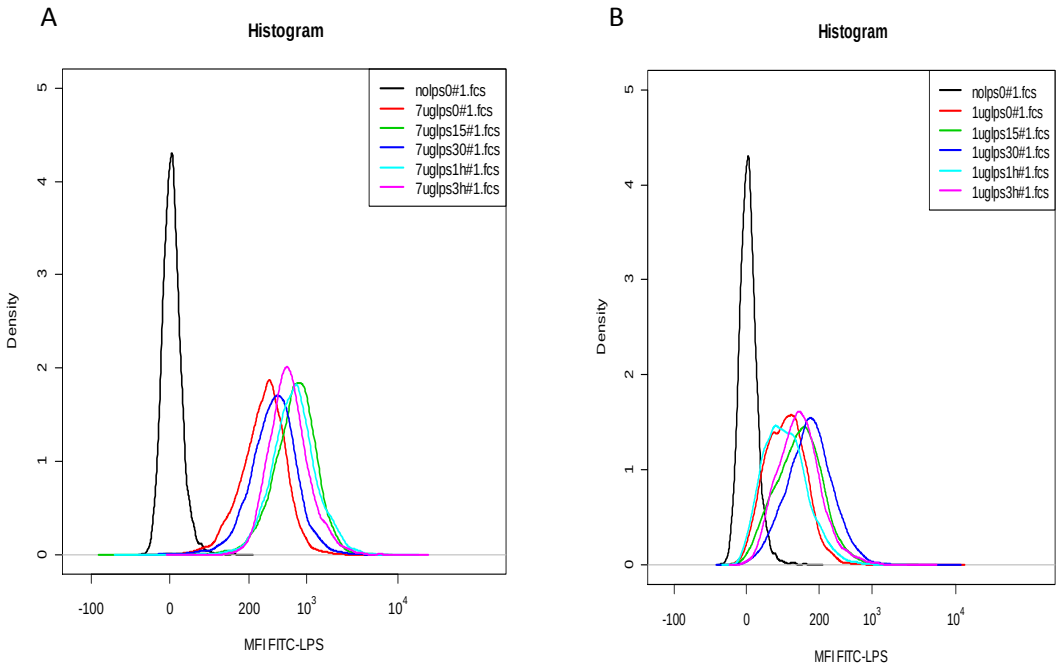

Figure 15. Histogram of LPS-TLR binding with time for 1 and 7 µg LPS. In A, Density distribution of the cells expressing fluorescence for 7 µg LPS ligand concentration is shown. In B, Density distribution of the cells expressing fluorescence for 1 µg LPS ligand concentration is shown. From A and B, it is clear that fluorescence intensity was higher for higher ligand.

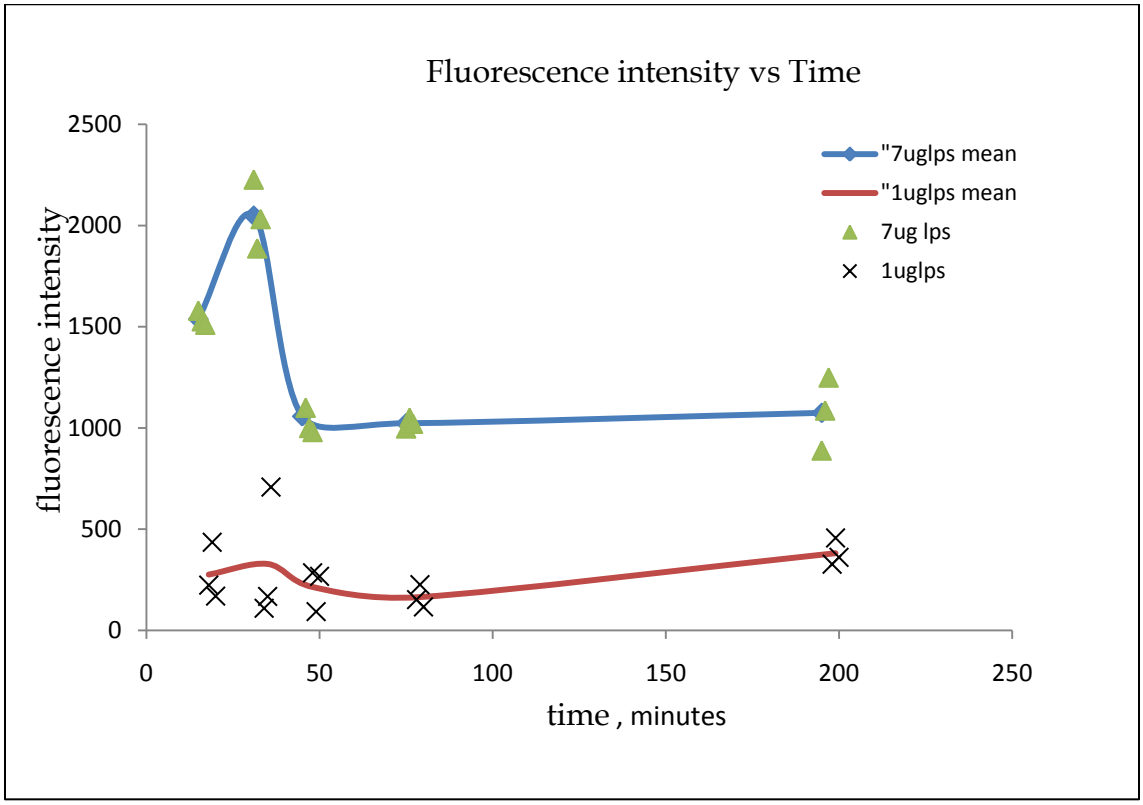

Figure 16. Dose response plot of LPS-TLR4 binding with respect to time. Triangles represent the fluorescent intensity response for 7 µg LPS with respect to time. Blue solid curve passing through the triangles represent the mean value of the corresponding data. Cross symbols represent the fluorescent intensity response for 1 µg LPS with respect to time. Brown solid curve represents the mean value of the corresponding data. The fluorescence intensity was observed to increase with time for both 1, 7 µM concentrations of FITC-LPS up to 30 minutes, then it decreased sharply and remained constant.

Chapter 4. Discussion

The molecular weight of LPS which was found to be close to 50 kDa using SDS-PAGE method, was in well agreement with the range it exhibits in the presence of SDS and heat treatment. And also, since critical aggregation concentration in culture medium could be different due to the binding of LPS to serum components such as LBP, sCD14, and lipoproteins we were able to determine the actual size of LPS using SDS-PAGE.

Table 5. Dissociation , nonspecific binding constant and Total Receptor concentration at 4 °C and 37 °C for LPS-TLR4 association

Constants	**4°C**	**37 °C**
$\mathbf{K_D}$	18 µM	56.3 µM
$\mathbf{R_{tot}}$	1800 MFI	2500 MFI
$\mathbf{K_{NS}}$	6.5 μM^{-1}	1.93 μM^{-1}

* MFI – mean fluorescence intensity

The Dissociation constant, K_D, non-specific binding constant and total receptor concentration for LPS-TLR4 binding at 4 °C and 37 °C are reported in Table 5. There has been much interest in the kinetics of receptor-ligand interactions, especially in the case of molecules involved in immune responses. [60] For the LPS-mouse TLR4/MD-2 interaction, the reported affinity was about 3-10 nM, this binding assay used immunoprecipitation and was different from conventional ligand binding assay. They could not directly compare the LPS interaction with TLR4-MD-2 or CD14 complexes because LPS was not coprecipitated with CD14 or MD-2 due to the presence of detergents.[61] The dissociation constant for LPS-human MD-2 interaction was reported as 65 nM.[62] The Dissociation constant for LPS-TLR4 interaction, reported by Shin et al. was 20 µM at 25 °C. Differences in assay sytems, interaction forces of molecules, may contribute to the observed differences. With affinities differing by three orders of magnitude, it is hard to rationalize the current model of LPS interaction with TLR4.

As, it is known that LPS does not interact with TLR4 alone, and it also binds to other receptor proteins significantly, we include non-specific binding term, accounting for the binding of LPS to its receptor proteins. Clearly, from Table 5, we can see that K_D and R_{tot} values are higher at 37 °C than that obtained at 4 °C, which was expected because at 37 °C, conditions are rigorous and LPS undergoes internalization along with its receptor. Trypan blue addition quenched the surface fluorescence obtained at both 4 °C and 37 °C, enabling us to quantify the fluorescence obtained by internalization and surface binding.

Time course experiments show gradual increase in fluorescence exhibition, up to 30 minutes, drops and levels off. This means, equilibrium binding was attained at 30 minutes which confirms that, the data obtained for LPS-TLR4 binding at both 4 °C and 37 with 30 minutes incubation period was at equilibrium. But non-specific binding constant was found to be higher for LPS-TLR4 binding at 4 °C than at 37 °C. As expected, the total receptor concentration was higher at 37 °C than that of obtained at 4 °C.

To determine the quantitative differences between the subpopulations of cells, and moreover, to give individual populations a subtle relevance, standards are necessary with known amounts of fluorescence to which these samples can be compared. In Figure 17. a microbead containing a fluorescent dye, fluorescein-isothio cyanate (FITC), is shown along with the cell labeled with same dye. If a series of such microbeads containing varying amounts of the fluorescent dye is run on a flow cytometer, the resulting distributions will be obtained as in Figure 18 indicated by “Bead1, Bead 2 and Bead 3”. Now if a cell population stained with same dye is also on flow cytometer under same conditions, then the fluorescence intensity of the cells can be quantitatively compared to those of the calibrated microbeads.

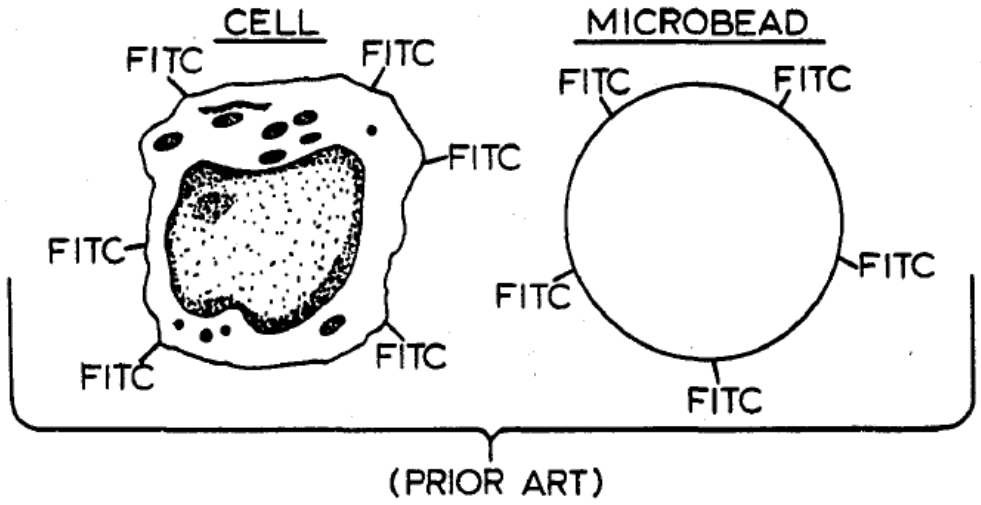

Figure 17. A microbead containing fluorescent labeled dye fluorescein isothiocyanate along with the cell labeled with same dye.[63]

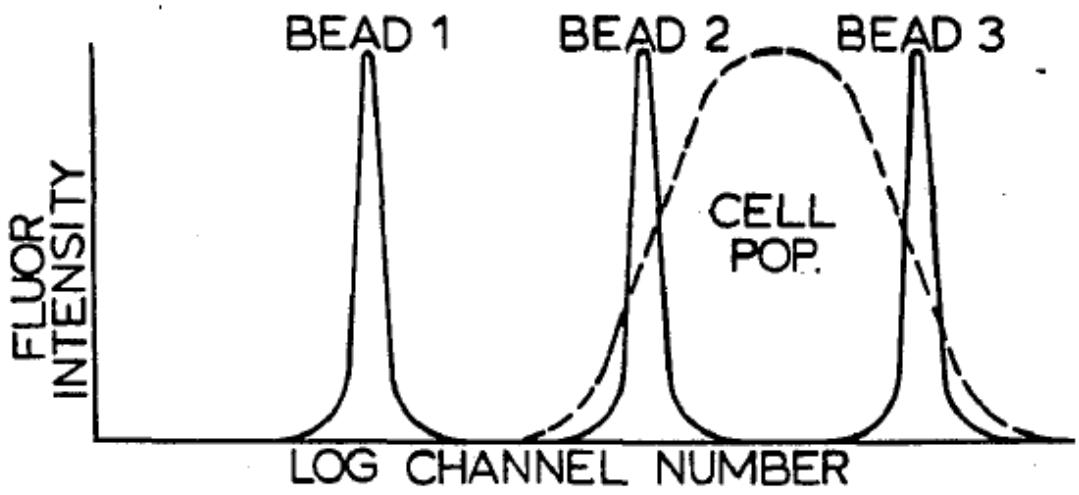

Figure 18. Fluorescent intensity distributions of the microbeads for different channels run on flow cytometer.[63]

The linear plot of FITC molecules versus mean fluorescence intensity obtained from the peaks obtained in the figure 18, quantitates the fluorescence to which the cell samples can be compared.

4.1. Conclusion

We conclude from the series of experiments conducted at 4 °C and 37 °C that dissociation constant for LPS-TLR4 was found to be 18µM and 56µM respectively. The non-specific binding constants obtained were 6.5μM^{-1} and 1.93 μM^{-1} at 4 °C and 37 °C respectively. The molecular weight of LPS was found to be 50 kDa using SDS-PAGE. At 37 °C, measured fluorescence was more than that measured at 4 °C, because of the internalization process. The fluorescence quenching observed at 37 °C and 4 °C using trypan blue was incomplete and imposed questions on occurrence of pinocytosis. The LPS-TLR4 binding with respect to time was found to increase up to certain time and become constant. The equilibrium binding time was observed to be around 30 minutes.

4.2 Future Work

In this study, non-specific binding of LPS to TLR4 in-vitro, was not inhibited. Inhibiton of non-specific binding of FITC-LPS to TLR4/MD-2 or CD14 can be done using blocking agents such as antibodies against TLR4 complexes, through which binding constants can be determined more accurately. And a model describing the interaction of FITC-LPS to TLR4/MD-2 complexes leading to a signaling cascade that induces the activation of transcription factors such as NF-□B. These transcription factors controls cell growth and cytokine production.

Chapter 5. Safety Considerations

1. Before using any chemical Material Safety Data Sheet (MSDS) is always to be reviewed.
2. Universal lab safety rules such as not eating, drinking or smoking in the laboratory are strictly to be followed.
3. In the laboratory open-toe shoes should not to be worn as they leave us vulnerable if there is a spill.
4. Always lab coat must be worn while performing experiment.
5. Suitable hand gloves must be used while performing experiment, against potentially dangerous materials.
6. Acquaintance with laboratory safety rules is necessary and should be very well aware of the location of first aid kit, the radiation and chemical spill kit, eyewash and safety showers.
7. Emergency phone numbers should be memorized to call upon in an emergency situation.

References:

1. http://www.ncbi.nlm.nih.gov/books/bv.fcgi?rid=imm.section.2367.
2. Aderem, A. A. underhill, D. M., 1999, Mechanisms of phagocytosis in macrophages *Annu. Rev. Immnunol.* **17**, 593-623.
3. P.R. Taylor, L.Martinez-Pomares, M. Stacey, H-H. Lin, G.D. Brown, and S.Gordon, *Annu.Rev. Imunol.* 2005, **23**:901-44.
4. Janeway, C. A., Medzhitov, R., 1998. The role of innate immunity in adaptive immune response. *Semin. Immunol. 10*, 349-350.
5. Rietschel,E.T. and O.Westphal. 1999. Endotoxin: Historical perspectives. *In* Endotoxin in Health and Disease. H.Brade, S.M.Opal, S.N.Vogel, and D.C.Morrison, editors. Marcel Dekker, Inc., New York. 1-30.
6. Hitchcock,P.J., L.Leive, P.H.Makela, E.T.Rietschel, W.Strittmatter, and D.C.Morrison. 1986. Lipopolysaccharide nomenclature - past, present, and future. *J Bacteriol* 166:699-705.
7. Ulevitch, R.J., Tobias, P.S., 1999. Recognition of Gram negative bacteria and endotoxin by the innate immune system. *Curr. Opin. Immunol*. **11**, 19-22.
8. Rietschel,E.T., L.Brade, B.Lindner, and U.Zahringer. 1992. Molecular biochemistry of lipopolysaccharides. *In* Bacterial Endotoxic Lipopolysaccharides. D.C.Morrison and J.L.Ryan, editors. CRC Press, Boca Raton,FL. 3-42.
9. Qureshi,N., K.Takayama, D.Heller, and C.Fenselau. 1983. Position of ester groups in the lipid A backbone of lipopolysaccharides obtained from *Salmonella typhimurium*. *J.Biol.Chem.* 258:12947-12951.
10. Raetz C.R. Whitfield C. *Annu. Rev. Biochem* 2002;**71** :635-700.
11. Raetz C.R.H, R.J.Ulevitch, S.D.Wright, C.H.Sibley, A.Ding and C.F.Nathan, 1991. Gram–negative endotoxin: an extraordinary lipid with profound effects on eukaryotic signal transduction. FASEB J. **5**: 2652-2660.
12. Calendra T., J.D. Baumgartner, G.F.Grau, M.M.Wu, P.H.Lambert, J.Schellekens, J.Verhoef and M.P.Glausner, 1990.Prognostic values of tumor necrosis factor cachectin, interleukin 1, interleukin-alpha and interferon-gamma in the serum of

patients with septic shock Swiss-Ditch J5 immunoglobulin study group J. Infect.Dis.**161**:982-987.

13. Creasey A.A, P.Stevens, J.Kenney, A.C.Allison, K.Warren, R.Catlett, L.Hinshaw, and F.B.J.Taylor,1991. Endotoxin and cytokine profile in plasma of baboons challenged with lethal and sublethal *Escherichia Coli*. Circ.Shock **33**:84-91.
14. Debets J.M, R.Kampmejjer, M.P.Van der Linden, W.A.Buurman, and C.J.van der Linden.1989.Plasma tumor necrosis factor and mortality in critically ill septic patients. Crit.Care.Med. **17**:489-494.
15. Raetz, C.R.H., 1990. Biochemistry of endotoxins. *Annu. Rev*. Biochem. **59**, 129-70.
16. Goyert, S.m., Ferrero, E.M., Seremetis, S.V., Winchester, R.J., Silver, J., Mattison, A.C., 1986. Biochemistry and expression of myelomonocytic antigens. *J.Immunol.***137**. 3909-3914.
17. Ferrero, E., Jiao, D., Tsuberi, B.Z., Tesio, L., Rong, G.W., haziot, A., Goyert, S.M., 1993. Transgenic mice expressing human CD14 are hypersensitive to lipopolysaccharide. *Proc.Natl. Acad. Sci*. USA **90**, 2380-2384.
18. Haziot, A., Ferrero, E., lin, X.Y, Stewart, C.L., Goyert, S.m., 1995. CD14-deficient mice are exquisitely insensitive to the effect of LPS. *Prog. Clin. Biol. Res*.**392**, 349-351.
19. Anderson, K.V., 2000. Toll signaling pathway in innate immune responses. *Curr. Opin. Immunol*. **12**, 13-19.
20. Akira S, Hemmi H. Recognition of pathogen-associated molecular patterns by TLR family. *Immunol Lett* 2003; **85**:85-95.
21. Medzhitov R, Janeway Jr CA. Innate immunity: the virtues of a nonclonal syatem of recognition. Cell 1997; 91:295-298.
22. Akira, S., Uematsu, S. & Takeuchi, O. Pathogen recognition and innate immunity. *Cell* **124**, 783-801 (2006).
23. Janeway, C.A.Jr & Medzhitov, R. Innate immune recognition. *Annu. Rev. Immunol*.**20**, 197-216 (2002).

24. Hirotani, T. *et al*. Regulation of lipopolysaccharide-inducible genes by MyD88 and Toll/IL-1 domain containing adaptor inducing IFN-□. *Biochem. Biophys. Res. Commun.* **328**, 383-392 (2005).
25. Barton, G.M, Kagan, J.C. & Medzhitov, R. Intracellular localization of Toll-like receptor 9 prevents recognition of self DNA but facilitates access to viral DNA. *Nat. Immunol*. **7**, 49-56 (2006).
26. Latz, E. *et al*. TLR9 signals after translocating from the ER to CpG DNA in the lysosome. *Nat. Immunol.* **5**, 190-198 (2004).
27. Hayashi, F. *et al*. The innate immune response to bacterial flagellin is mediated by Toll-like receptor 5. *Nature* **410**, 1099-1103 (2001).
28. Toshchakov, V. *et al*. TLR4, but not TLR2, mediates IFN-□-induced STAT1□/□-dependent gene expression in macrophages. *Nat. Immunol*. **3**, 392-398 (2002)
29. Alexopoulou, L., Holt, A.C., Medzhitov, R. & Flavell, R.A. Recognition of double-stranded RNA and activation of NF-□B by Toll-like receptor 3. *Nature* **413**, 732-738 (2001).
30. Lund, J.m. *et al*. Recognition of single-stranded RNA viruses by Toll-like receptor 7. *Proc. Natl. Acad. Sci.* USA **101**, 5598-5603 (2004).
31. Diebold, S.S., Kaisho, T., Hemmi, H., Akira, S. & Reis e Sousa, C. Innate antiviral responses by means of TLR7-mediated recognition of single stranded RNA. *Science* **303**, 1529-1531 (2004).
32. Barton, G.M. & Medzhitov, R. Toll-like receptor signaling pathways. *Science* 300, 1524-1525 (2003).
33. O'Neill, L.A. & Bowie, A.G. The family of five; TIR-domain-containing adaptors in Toll-like receptor signaling. *Nat. Rev. Immunol*. **7**, 353-364 (2007).
34. Kate A. Fitzgerald *et al.* Journal of Endotoxin Research, *Vol. 9*, No.**6**, 2003.
35. Kitchens RL, Wang P, Munford RS. Bacterial lipopolysaccharide can enter monocytes via two CD14-dependent pathways. *J Immunol* 1998; **161**:5534-5545.

36. Nagai Y, Akashi S, Nagafuku M et al. Essential role of MD-2 in LPS responsiveness and TLR distribution. *Nat Immunol* 2002;**3**: 667-672.
37. Thieblemont N, Wrigt SD. Transport of bacterial lipopolysaccharide to the Golgi apparatus. *J Exp Med 1999*; **190**: 523-534.
38. Hornef MW, Frisan T, Vandewalle A, Normark S, Ritcher-Dahlfors A. Toll-like receptor 4 resides in the Golgi apparatus and colocalizes with internalized lipopolysaccharide in intestinal epithelial cells. *J Exp Med* 2002; **195**:559-570.
39. Jann, B., *et al*., Heterogeneity of lipopolysaccharide chain lengths by sodium dodecylsulfatepolyacrylamide gel electrophoresis. *Eur. J. Biochem*., **60**, 239-246 (1975).
40. Leive, l., and Morrison, D.C., Isolation of LIpopolysaccharides from bacteria. *Methods in Enzymology*, **28**, 254-263 (1972).
41. Hirotaka Sasaki and Stephen H.White *Biophysical Journal Volume* 95 July 2008 986-993.
42. Mueller, M., B. Lindner, S. Kusumoto, K. Fukase, A.B. Schromm, and U. Seydel. 2004. Aggregates are the biologically active units of endotoxin *J. Biol.Chem*.**279**;26307-26313.
43. Takayama, K., D.H.mitchell, Z.Z. Din, P.Mukerjee, C.Li, and D.L. Coleman, 1994. Monomeric Re lipopolysaccharide from Escherichia coli is more active than the aggregated form in the limulus amebocyte lysate essay and in inducing Egr-1 m-RNA in murine peritoneal macrophages. *J. Biol. Chem*. **269**; 2241-2244.
44. Ulevitch, R.J., and P.S. Tobias. 1995. Receptor-dependent mechanisms of cell stimulation by bacterial endotoxin. *Annu. Rev. Immunol*.13;437-457.
45. Miyake, K.2004. Innate recognition of lipopolysaccharide by Toll-like receptor 4-MD-2. *Trends Microbiol.* 12:186-192.
46. Rivera et al., Journal of bacteriology, Feb. 1988, p. 512-521 Vol. 170, No.2.
47. A. Pichlmair and C. Reis e Sousa, Innate recognition of viruses, *Immunity* **27** (2007), pp. 370–383.

48. B. Beutler and E.T. Rietschel, Innate immune sensing and its roots: the story of endotoxin, *Nat Rev Immunol* **3** (2003), pp. 169–176.
49. Ha Jae Shin, Hayyoung Lee, Jong dae Park, Hak Chul Hyun, Hyung Ok Sohn, Dong Wook Lee, and Young Sang Kim, April 16, 2007; *Mol. Cells*, Vol. **24**, No. 1, pp. 119-124.
50. Loike JD, Silverstein SC, *J. Immunol methods*, 1993 feb 25; **57**(1-3)373-9.
51. Sahlin S, Hed J, Rundquist I. J. *Immunol methods* 1983 May 27; **60**(1-2):115-24.
52. Linderman JJ. Kinetic modeling approaches to understanding ligand efficacy. In: Kenakin T, Angus JA, Black JW, Barr AJ, editors. The pharmacology of functional, biochemical,a nd recombinant receptor systems. Handbook of experimental pharmacology. New York: Springer-Verlag; 2000. P 119-146.
53. Lauffenburger DA, Linderman JJ, Receptors: models for binding, trafficking, and signaling. New York: Oxford University Press; 1993. 365 p.
54. Sklar LA, Jesaitis AJ, Painter RG, Cochrane CG. LIgand/receptor internalization: a spectroscopic analysis and acomparison of ligand binding. Cellular response, and internalization by human neutrophils. J Cell Biochem 1982; 20:193-202.
55. Thomas J.F. Nieland*, Marsha Penman*, Limor Dori, Montey Kreiger and Tomas Kirchhausen, Dicovery of chemical inhibitors of the selective transfer of lipids mediated by the HDL receptor SR-BI. PNAS,November 26,2002, vol.99,no.24 15422-15427.
56. Sklar LA, Finney DA. Analysis of ligand-receptor interactions with the fluorescence activated cell sorter. Cytometry 1982; 3: 161-165.
57. Hoffman JF, Keil ML, Riccobene TA, Omann GM, Lindermann JJ. Interconverting receptor states at 4 degrees C for the neutrophil N-formyl peptide receptor. Biochemistry 1996; 35:13047-13055.
58. Klinke, D. J. *; Brundage, K. M. ; "Scalable analysis of flow cytometry data using R/Bioconductor", cytometry A 75 (2009) 699-706
59. Van Amersfoot ES, Van Strijp JA. Evaluation of a flow cytometric fluorescence quenching assay of phagocytosis of sensitized sheep erythrocytes by

polymorphonuclear leukocytes. Wiley Interscience March 8, 2005, Volume 12 Issue 4, pages 294-301.

60. Vales-Gomez, M., Reyburn, H. T., Mandelboim, M., and Strominger, J. L. (1998) Kinetics of interaction of HLA-C ligands with natural killer cell inhibitory receptors. *Immmunity* **9**, 337-344.
61. Akashi, S., Saitoh, S., Wakabayashi, Y., Kikuchi, T., Takamura, N., et al. (2003) Lipopolysaccharide interaction with cell surface Toll-like receptor 4-MD-2: higher affinity than that with MD-2 or CD-14. *J. Exp. Med*. **198**, 1035-1042.
62. Viriyakosol, S., Mathison, J. C., Tobias, P. S., and Kirkland, T. N. (2000) Structure-function analysis of CD14 as a soluble receptor for lipopolysaccharide. *J. Biol. Chem*. **275**, 3144-3149.
63. Abraham Schwartz, Durham, NC, Fluorescent calibration microbeads simulating stained cells, patent number 4,714, 682, filed April 3, 1987.